Attachment 7

CDM Apvd

RELEASED FOR USNRC REVIEW 2018/01/26

30441R00032
Revision C

REACTOR-BASED MOLYBDENUM-99 SUPPLY SYSTEM PROJECT

RELAP ACCIDENT ANALYSIS AND FRAPTRAN TARGET ROD TRANSIENT ANALYSIS DESIGN CALCULATION REPORT

Prepared by General Atomics
for the U.S. Department of Energy/National Nuclear Security Administration and Nordion Canada Inc.

Cooperative Agreement DE-NA0002773

[redacted]

GA Project 30441
WBS 1160

GENERAL ATOMICS

MURR® Matters...

nordion

REVISION HISTORY

Revision	Date	Description of Changes
A	01NOV16	Information Issue Initial Release
B	27JAN17	RELAP5 model revision and new accident analyses
C	26JAN18	New analysis with revised tolerances, cladding and pellet roughness, and gas gap composition

POINT OF CONTACT INFORMATION

PREPARED BY:			
Name	**Position**	**Email**	**Phone**
J. Bolin	Engineer	John.Bolin@ga.com	858-455-2467
R. Hon	Engineer	Ryan.Hon@ga.com	858-455-4374
APPROVED BY:			
Name	**Position**	**Email**	**Phone**
B. Schleicher	Chief Engineer	Bob.Schleicher@ga.com	858-455-4733
K. Murray	Project Manager	Katherine.Murray@ga.com	858-455-3272
K. Partain	Quality Engineer	Katherine.Partain@ga.com	858-455-3225

DESIGN CONTROL SYSTEM DESCRIPTION

		DISC	QA LEVEL	SYS
☐	R & D			
☒	DV&S			
☐	DESIGN			
☐	T&E	N	I	N/A
☐	NA			

TABLE OF CONTENTS

LIST OF FIGURES

[redacted]

LIST OF TABLES

ACRONYMS

Acronym	Description
ANL	Argonne National Laboratory
BOL	Beginning of Life
CHF	Critical Heat Flux
CHFR	Critical Heat Flux Ratio
DHRS	Decay Heat Removal System
EOL	End of Life
GA	General Atomics
HX	Heat Exchanger
ID	Inner Diameter
LEU	Low Enriched Uranium
LOCA	Loss of Coolant Accident
LOFA	Loss of Flow Accident
LOPF	Loss of Pump Flow
LSSS	Limiting Safety System Setting
LWR	Light Water Reactor
MTU	Metric Ton Uranium
MURR	University of Missouri Research Reactor
OD	Outer Diameter
pcm	per cent mille = 10^{-5}
PNNL	Pacific Northwest National Laboratory
SAR	Safety Analysis Report
SGE	Selective Gas Extraction
SI	Systeme International (metric units)
TA	Target Assembly
TCS	Target Cooling System
USNRC	United States Nuclear Regulatory Commission

1 OBJECTIVE

The objective of this report is to analyze and present the results of transients and potential accidents associated with the irradiation of target rods for the production of the medical isotope Mo-99. The target rods utilize low enriched uranium (LEU) to produce Mo-99 as a fission product, which is then extracted from the target rod post-irradiation for use in medical diagnostic procedures. The LEU targets will be irradiated in the reflector region of the University of Missouri Research Reactor (MURR). The target assembly to be installed in the reflector region will be equipped with its own independent cooling system, both for normal cooling of the rods during routine operation, as well as a natural circulation cooling system that will provide the required cooling to the LEU target rods in the case of a loss of flow or loss of coolant accidents. The normal cooling system draws and discharges its cooling water from and to the MURR pool.

1.1 Analysis Objectives for Reactivity Transients

Two reactivity transients were analyzed: rapid insertion of positive reactivity, and control blade withdrawal. The reactivity transient is driven by the MURR core and is defined in the MURR Safety Analysis Report (SAR) submitted for relicensing (References 1 and 2). The steady-state conditions of the target rod are calculated by FRAPCON which determines thermal expansion, pellet-clad interaction, pellet relocation, and fission gas release as described in Section 3.2. While FRAPCON can calculate the thermal boundary condition of the target rod, it was determined that heat transfer calculation assumes that the water properties are at the high pressures and temperatures typical of light water reactors and therefore not suitable for the low pressures and temperatures within the target assembly. For this reason, the thermal boundary conditions in FRAPCON are defined by steady state RELAP5 runs at the appropriate power and flow conditions. FRAPCON results are then used as input to a transient FRAPTRAN run which simulates the reactivity transient. The objectives of the FRAPTRAN analysis are to assess cladding strain due to internal pressure and pellet-clad interaction, to assess peak pellet temperature, and to determine minimum critical heat flux ratio.

1.2 Analysis Objectives for Loss of Target Coolant and Loss of Target Flow

The loss of target coolant and loss of target flow accidents are analyzed with a RELAP5 model that includes both target assemblies (30441D00211, 30441D00207, 30441D00210, 30441D00308, 30441D00313, 30441R00031), the reactor pool, the complete target cooling system, and the target decay heat removal system (30441R00019). The model includes the target cooling system pump and heat exchanger, and target decay heat removal system (DHRS) valves needed for the transition from normal to natural circulation cooling flow. The target cooling system is depicted in Figure 1. The RELAP5 analyses are used to assess the performance of the cooling systems both with and without the target DHRS valves operating, to assess changes

in cladding and pellet temperatures, and to determine minimum critical heat flux ratio (CHFR) using thermal hydraulic results from the accident simulation.

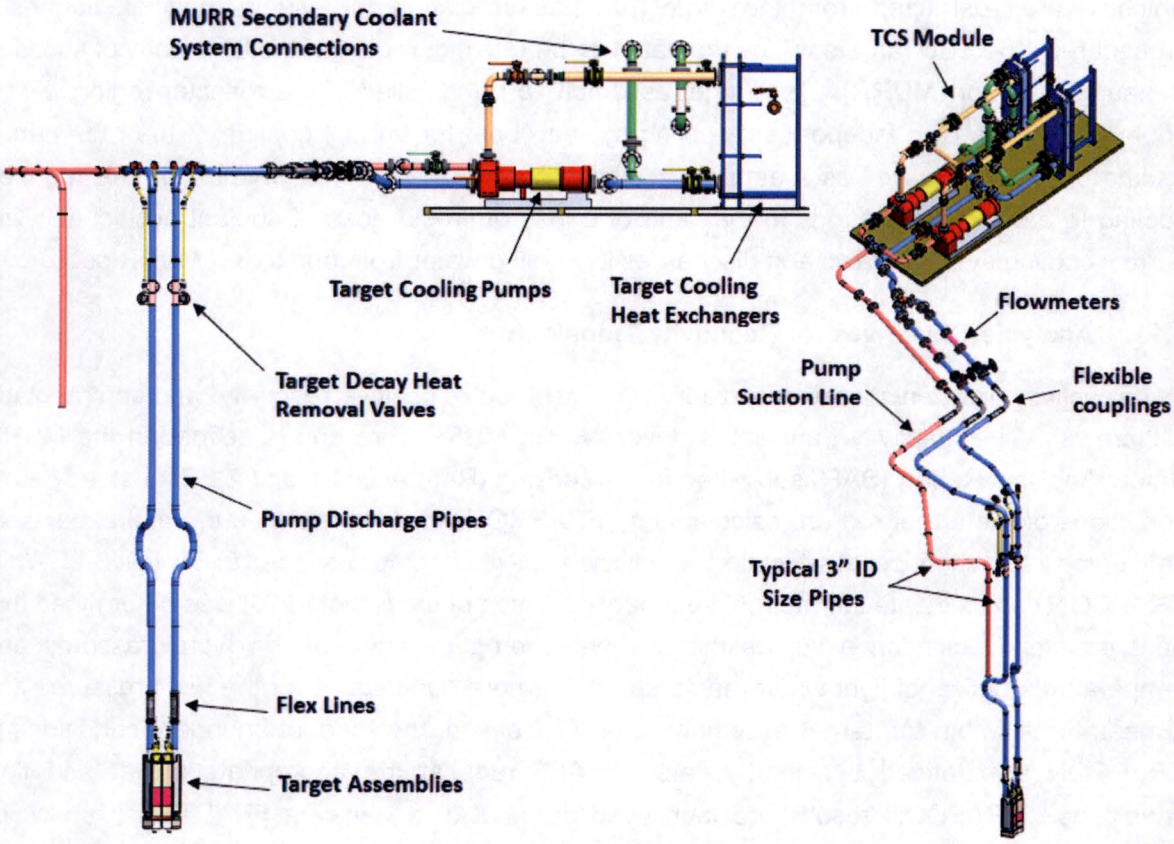

Figure 1. Target cooling system

2 APPLICABLE DOCUMENTS

A list of applicable documents is provided below.

DOCUMENT NUMBER	DOCUMENT TITLE
30441D00207	Target System Cladding
30441D00210	Target Rod Assembly
30441D00211	Target System Pellet
30441D00308	Retaining Spring, Target Rod Assembly
30441D00313	Body, TR Cartridge
30441R00019	Target System Cooling Calculation Report
30441R00024	RELAP (Version 5 Mod 3.3 P03) Software Verification Test Report
30441R00025	FRAPCON (Version 4.0 Patch 1) Software Verification Test Report
30441R00026	FRAPTRAN (Version 2.0) Software Verification Test Report
30441R00031	Mo-99 Target Assembly Nuclear Design for Once-Through Operation
30441R00038	Computational Fluid Dynamics Analysis Of Target Housing Design Calculation Report

3 METHODS

3.1 RELAP5

The transient analysis code RELAP5 (Reference 3) has been developed for the United States Nuclear Regulatory Commission (USNRC) to provide analysis to support rulemaking, licensing audit calculations, evaluation of accident mitigation strategies, evaluation of operator guidelines, and experiment planning analysis. The version RELAP5/MOD3.3 was developed jointly by the NRC and a consortium of several other organizations with the goal of developing a code suitable for the analysis of all transients and accidents in light water reactor (LWR) systems.

RELAP5 is a standard tool used by the nuclear industry for the analysis of LWR systems. The code models the behavior of the reactor core and cooling system for various transient situations including loss of coolant, transient without scram, loss of offsite power, loss of feed water, and loss of flow. There has been extensive verification and validation (Reference 3) of the code which gives confidence in the quality of its results. While developed for light water reactor analysis, the code is also general enough to simulate a wide variety of thermal hydraulic systems containing mixtures of water, steam, noncondensables, and solute.

The hydrodynamic model in RELAP5 is a one-dimensional, transient, two-fluid model for flow of a two-phase steam-water mixture that can contain noncondensable components in the steam phase and a soluble component in the water phase. The two-fluid equations of motion used in the model are formulated in terms of volume and time averaged parameters of the flow. Transverse flow effects, such as friction and heat transfer, are formulated in terms of bulk properties using empirical transfer coefficient formulations. Additionally specific models have been developed for particular flow situations. The system model is solved numerically using a semi-implicit finite-difference technique.

For heat transfer across boundaries, RELAP5 makes use of heat structures. Heat structures are represented by one-dimensional heat conduction in rectangular, cylindrical, or spherical geometry. The code is able to model a variety of heat transfer situations including fuel pins with nuclear heating, conduction between pipe walls, and heat transfer across steam generator tubes. The time dependence of heat sources can be inputted by the user or obtained from reactor kinetics and various boundary conditions can be used. The heat structures surfaces connected to hydrodynamic volumes contain correlations for convective, nucleate boiling, transition boiling, and film boiling heat transfer from the wall to the water as well as heat transfer from the water to the wall including condensation.

Control systems are provided within the code to model events in transient situations. Parameters at certain points in the system can be used to cause events elsewhere to happen. For example these features can be used to cause a pump to trip or a valve to open at a certain point in time.

The power behavior of a nuclear reactor can be modeled using the included point reactor kinetics model. This model computes both immediate power from fission and neutron moderation as well as decay power from the fission products undergoing radioactive decay. The model is adequate in situations where the spatial power distribution remains constant. The user has a choice of which decay power model to use. A detailed description of the models and methods used in RELAP5 can be found in the user's manual (Reference 3). GA has verified the code for use on this project (30441R00024).

3.2 FRAPCON

FRAPCON-4.0 (Reference 4) is a steady state fuel performance code developed by Pacific Northwest National Laboratory (PNNL) for the USNRC. The code has been developed for calculating LWR fuel behavior up to a rod average burnup of 62 gigawatt days per metric ton of uranium (GWd/MTU). The code calculates only "steady-state" situations, including slow power ramp ups and long periods of constant power, typical to that of LWR operation. A number of parameters significant for fuel rod analysis are calculated by the code including fuel and cladding temperatures, cladding hoop strain, cladding oxidation, hydriding, fuel irradiation swelling, fuel densification, fission gas release, and rod internal gas pressure. The code can also be used to

generate the initial conditions required for transient fuel behavior analysis with the FRAPTRAN code.

FRAPCON uses an iterative process to calculate all of the interrelated effects of fuel rod performance. A typical calculation will start by computing the initial conditions of the problem from the inputs given. The temperature distribution throughout the fuel rod will then be computed. Given the temperature distribution, any deformations to the fuel and cladding will be calculated. The deformation of the fuel and cladding will cause differences in the rate of heat transfer throughout the rod, requiring the fuel temperature distribution and deformation to be iterated upon until the gap temperature difference has converged. Next the fission gas release and gas pressure are computed for the rod. This change in gas pressure will have an effect on the temperature distribution of the rod. Another iterative loop is used until the gas pressure in the rod is converged after which time is advanced to the next step.

The material properties used in FRAPCON come from a database that relates important system and material properties to one another. For example, the fuel thermal conductivity is a function of temperature, density and burnup and the cladding stress-strain relationship is a function of temperature, strain rate, cold work, and neutron fluence. There are various models and methods that the code uses in order to calculate pellet redistribution, gas release, crud disposition, etc., some of which the user can specify for specific problems. A detailed description of the methods and models used in FRAPCON can be found in the user's manual (Reference 4). GA has verified the code for use on this project (30441R00025).

3.3 FRAPTRAN

FRAPTRAN-2.0 (Reference 5) is a code developed by PNNL for the USNRC that calculates the performance of LWR fuel rods during transient and accident situations. These accident conditions for pressurized water reactors include reactivity-initiated accidents and loss-of-coolant accidents. For these situations, FRAPTRAN models heat conduction, heat transfer from cladding to coolant, elastic/plastic fuel and cladding deformation, cladding oxidation, fission gas release, and fuel rod gas pressure. FRAPTRAN does not model fuel densification, fuel swelling, cladding creep, and cladding irradiation growth, which vary slowly with time. These parameters are obtained from the FRAPCON code, which uses the same materials database, to set the conditions at the start of the transient.

In order to calculate a solution, FRAPTRAN begins with calculating the temperatures of the fuel and cladding followed by the fuel rod gases. Next the stresses and strains on the fuel and cladding are calculated. Then the fission gas release and gas pressure are calculated. Since the temperatures, pressures, and stresses are all related to one another they are iterated upon until the temperature profile converges. After the temperature converges cladding oxidation and ballooning are calculated.

FRAPTRAN uses finite difference techniques to calculate the variables which influence fuel rod performance. These variables are calculated at different user defined radial and axial positions with different axial positions taken to be independent of one another (stacked one-dimensional solution). A detailed description of the methods and models used in FRAPTRAN can be found in the user's manual (Reference 5). GA has verified the code for use on this project (30441R00026).

4 ASSUMPTIONS

4.1 RELAP5 Generic Code Assumptions

RELAP5 is designed for use in analyzing the interactions of system components and does not provide detailed simulations of fluid flow within components. It therefore has limited capabilities in modeling multi-dimensional effects in heat transfer, fluid flow, and reactor kinetics. Some of the major assumptions present in the code are as follows:

- One dimensional flow with cross-flow junctions to allow some multi-dimensional effects
- Limited geometry specification of components, with a coarse nodalization scheme
- One dimensional heat flux
- Point reactor kinetics

For a more detailed analysis of all the assumptions involved with RELAP5 the reader is encouraged to consult the code manual (Reference 3).

4.2 FRAPCON Generic Code Assumptions

FRAPCON-4.0 has been developed specifically for the analysis of oxide fuel rods in light water reactors. As such there are some limitations inherent within the code due to the scope of the problem analyzed. The following are a list of those limitations:

- The code is limited to uranium oxide fuel types namely: uranium dioxide (UO_2), mixed oxide ($(U,Pu)O_2$), urania-gadolinia (UO_2-Gd_2O_3), and uranium dioxide with zirconium diboride (ZrB_2) coatings.
- The cladding is limited to Zircaloy-2, Zircaloy-4, M5, ZIRLO, and Optimized ZIRLO.
- The conditions of the system analyzed should be similar to those found in typical light and heavy water reactor systems.
- The code utilizes models based on steady state conditions.

- Gas release models are based upon slow power ramp data on the order of 0.1 days or greater and do not reflect the release rates for situations with rapid power changes. Rapid power changes are analyzed using FRAPTRAN.

- Only small cladding deformations can be calculated (<5% strain).

Additionally the code has been found to slightly over predict the cladding strain when under 65 GWd/MTU burnup (Reference 4).

For the calculation of heat transfer within the code, the following assumptions are as used:

- Heat conduction is ignored in the axial direction. This is a common assumption for systems with a large length to diameter ratio.

- Heat conduction in the azimuthal direction is ignored. This is a common simplification in nuclear safety analyses.

- During each time step boundary conditions are held constant.

- Steady-state flow is assumed.

- Fuel rod is modeled as a right circular cylinder surrounded by water as a coolant.

- The radial power profile within a fuel pellet is based off of fuel type, reactor type, and burnup.

For the cladding deformation model the following assumptions are used:

- Incremental theory of plasticity

- Prandtl-Reuss flow rule

- Isotropic work-hardening

- Thick wall cladding (thick wall approximation formula is used to calculate stress at mid-wall)

- No axial slippage at the fuel/cladding interface

- Bending strains and stresses in cladding are negligible and beyond the scope of the computer code

- Axisymmetric loading and deformation of cladding

[redacted]

The fuel deformation model is based upon the following assumptions:

- Thermal expansion, swelling, and densification are the only sources for fuel deformation
- No resistance to expansion of fuel
- No creep deformation of fuel
- Isotropic fuel properties

Lastly, the assumptions specific to the internal gas pressure model are:

- The perfect gas law is applicable (PV = nRT).
- Gas pressure is the same throughout the fuel rod due to interconnected gaps and cracks.
- Gas in the fuel cracks is at the average fuel temperature.

4.3 FRAPTRAN Generic Code Assumptions

FRAPTRAN-2.0 uses the results from FRAPCON to obtain starting conditions for transient calculations and has many of the same assumptions. However, new assumptions are needed as the system analyzed is no longer at steady-state. The major assumptions of the FRAPTRAN code not included in, or different from the FRAPCON assumptions, are as follows.

For the heat transfer model the following assumptions are used for the transient calculation in addition to the steady state assumptions from FRAPCON:

- Steady-state critical heat flux (CHF) correlations are assumed to be valid during transient conditions.
- Steady-state cladding surface heat transfer correlations are assumed to be valid during transient conditions.
- The coolant in the system is water or another coolant that can be modeled with altered heat transfer coefficients.

For the calculation of the plenum temperature for transient conditions the model is based on the following assumptions:

- The temperature of the top surface of the fuel stack is independent of the plenum gas temperature.
- The plenum gas is well mixed by natural convection.

- Axial temperature gradients in the spring and cladding are small.

The clad deformation model has the following assumptions different from FRAPCON:

- No low-temperature creep deformation of cladding
- Thin wall cladding (uniform temperature, stress and strain)

Lastly, the transient fuel rod gas pressure model is based off of the following assumptions:

- The gas behaves as a perfect gas.
- The gas flow past the fuel column is a quasi-steady process.
- The gas flow is compressible and laminar.
- The gas flow past the fuel column can be analyzed as Poiseuille flow (force balance only).
- Gas expansion in the plenum and ballooning zone is an isothermal process.
- The entire fuel-cladding gap can be represented as one volume containing gas at a uniform pressure.
- The flow distance is equal to the distance from the plenum to the centroid of the fuel-cladding gap.
- The minimum cross-sectional area of flow is equivalent to an annulus with inner radius **equal to that of the fuel pellet radius and a radial thickness of 25 µm** (0.98 mil).

4.4 Reactivity Transient Model Assumptions

For both reactivity transients, the power transient in the target rods is assumed to be proportional to the power transient in the MURR core. The power distribution in the target rods during the reactivity transients is assumed to be the same as the steady-state power distribution. The reactivity transients were assumed to occur either at the beginning or end of a three-week irradiation in which mid-week shutdowns also occur.

4.5 Loss of Target Coolant Model Assumptions

Because the target cooling system operates at a relatively low pressure of around 2 atm (0.202 MPa), a high pressure pipe break is not credible. A mechanical deformation due to some heavy object striking the cooling water pipe is assumed to be credible and that it would take at least 0.5 seconds for the pipe to be dislocated enough to form an offset break. Two worst-case

hypothetical break locations out of the reactor pool are analyzed: before the wye which affects both target assemblies, and at the joint after the last flex pipe before the cooling line enters the reactor pool. One break location within the reactor pool is analyzed at the joint connecting the flex pipe to the target assembly inlet pipe. These break locations are explained in more detail in Section 6.

Only one target DHRS valve is assumed to be open in each target cooling line. Analyses are also performed where none of the target DHRS valves operate to prove that they are not needed. RELAP5 only models gap closure due to thermal expansion so it overpredicts peak pellet temperatures. Therefore, RELAP5 is only used to predict changes in peak pellet temperature and FRAPCON is used to predict steady state peak pellet temperatures.

4.6 Loss of Target Flow Model Assumptions

The assumed pump characteristics, particularly its inertia and torque requirements, determine the coastdown of the pump. No flywheel or other special means are assumed which would extend the coastdown of the pump.

Only one valve is assumed to be open in each target cooling line. Analysis was also performed where none of the target DHRS valves operate to prove that they are not needed. RELAP5 only models gap closure due to thermal expansion so it overpredicts peak pellet temperatures. Therefore, RELAP5 is only used to predict changes in peak pellet temperature and FRAPCON is used to predict steady state peak pellet temperatures.

5 INPUTS

5.1 Target Pellet, Cladding and Cartridge Data

Pellet dimensions are explicitly provided as input for both FRAPCON and FRAPTRAN and are used to determine pellet volume and initial gap between pellet and cladding for RELAP5. Pellet and cladding dimensions and tolerances obtained from two drawings are used to provide necessary inputs and establish minimum and maximum gaps between the pellet and cladding (30441D00211 and 30441D00207). Pellet dimensions are depicted in Figure 2 and cladding dimensions are depicted in Figure 3. The minimum gap of [redacted] occurs when the maximum pellet outer diameter (OD) is matched with the minimum cladding inner diameter (ID). Similarly, the maximum gap of [redacted] occurs when the minimum pellet OD is matched with the maximum cladding ID. The nominal gap of 50 µm (1.97 mil) occurs with nominal pellet and cladding dimensions. Table 1 gives the pellet and cladding dimensions that are used in the minimum, nominal and maximum gap cases. The maximum cladding thickness was used in the minimum gap case to maximize cladding strain. The maximum cladding thickness was used in the maximum gap case to maximize pellet temperature. The nominal gap dimensions are used

to model the average of the remaining rods in both the minimum and maximum gap cases that are not explicitly modeled.

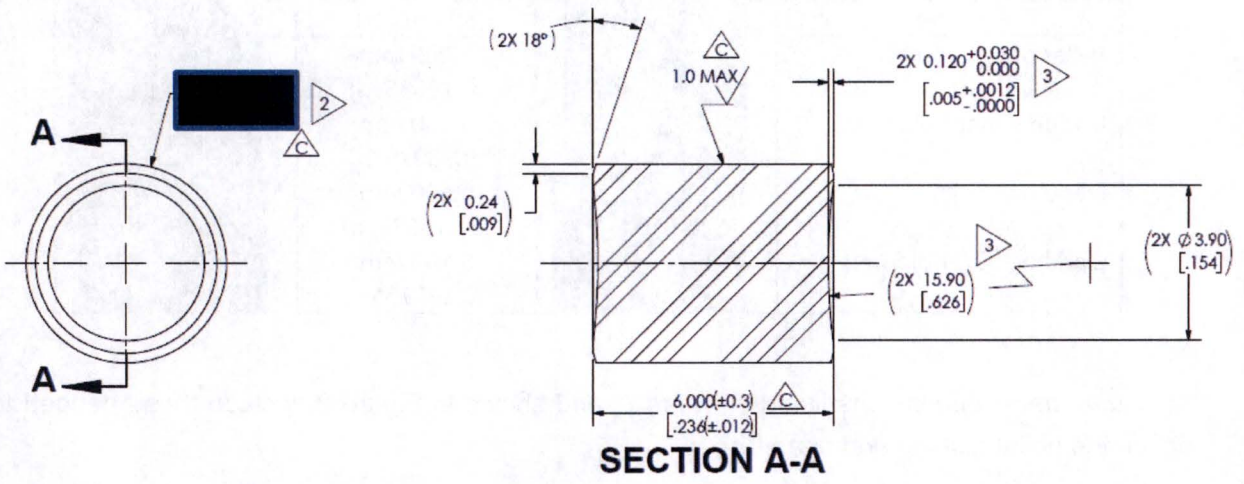

5a, b, f

Figure 2. Target pellet dimensions

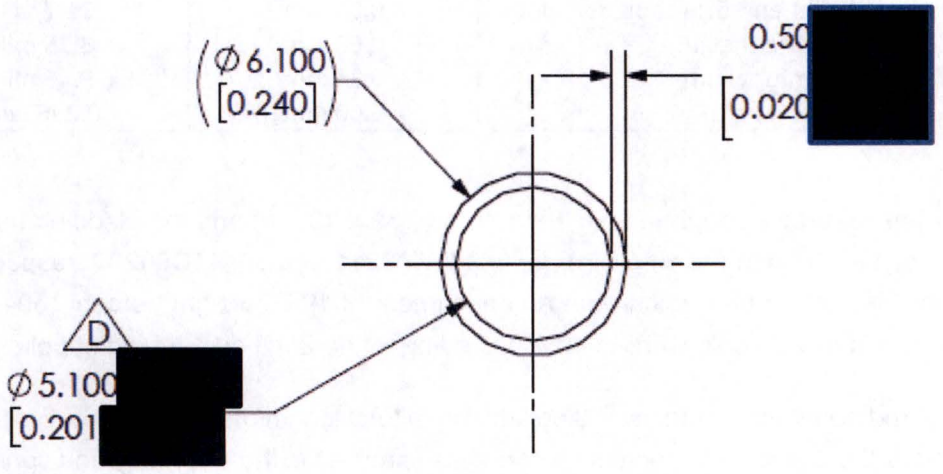

5a, b, f

Figure 3. Cladding dimensions

Table 1 Target Pellet and Cladding Dimensions

Parameter	[redacted]	50 µm gap	[redacted]
Pellet outer diameter		5.000 mm (0.19685 in)	
Cladding inner diameter		5.100 mm (0.20079 in)	
Cladding thickness		0.500 mm (0.019685 in)	
Cladding outer diameter		6.100 mm (0.24016 in)	

5a, b, f

Additional pellet dimensions listed in Table 2, and shown in Figure 2, include those needed to define the pellet dishing and chamfer.

Table 2 Additional Target Pellet Dimensions

Parameter	Dimension (SI)	Dimension (US)
Pellet dish depth	0.12 mm	4.72 mil
Pellet end-dish shoulder width	0.55 mm	21.7 mil
Chamfer height	0.08 mm	3.15 mil
Chamfer width	0.24 mm	9.45 mil
Pellet height	6.00 mm	0.2362 in

The pellet has a surface roughness of 1 x 10^{-3} mm (39 x 10^{-6} in) and the cladding has a surface roughness of 1 x 10^{-3} mm (39 x 10^{-6} in) per 30441D00211 and 30441D00207, respectively. The pellet density is 95% of theoretical with an enrichment of 19.75 weight percent (30441D00211). The cladding will have a cold work of 40% according to the Zircaloy-4 tubing supplier.

Each target rod nominally contains 100 pellets with a total length of 60.0 cm (23.62 in). The upper plenum above the pellet stack contains a spring as specified in the assembly and spring drawings (30441D00210 and 30441D00308, respectively). Table 3 presents the relevant spring and plenum data used for input.

Each target rod cartridge contains 11 target rods with a pitch of 1.163 cm (0.458 in) (30441D00313). The nominal diameter of the coolant holes in the cartridge is 1.445 cm (0.569 in) but an upper limit of 1.483 cm (0.584 in) was used which conservatively increases the flow area and reduces the flow velocity within the target cartridge.

[redacted]

Table 3 Target Spring and Plenum Data

Parameter	Value
Plenum length cold	3.9116 cm (1.54 in)
Plenum spring outer diameter	0.4826 cm (0.19 in)
Plenum spring wire diameter	0.635 mm (0.025 in)
Plenum spring number of turns	17
Rod fill gas pressure	101325 Pa (1 atm)
Rod fill gas	95% He, 5% Air

For all three gap sizes and associated cladding outer diameter (OD), the flow area, equivalent hydraulic diameter, and equivalent heated diameter were calculated using MATHCAD. The calculations depend on the location of the target rods because the corner rods differ from the interior rods within the target cartridge with respect to power profile. The results of these calculations are presented in Table 4 and are used primarily in the RELAP5 input but also in the FRAPCON and FRAPTRAN input for target rod 17. In target assembly 1, the maximum power rod and maximum power density rod are both interior rods so that the remaining rods are two corner rods and seven interior rods. In target assembly 2, the maximum power rod is a corner rod and the maximum power density rod is an interior rod so that the remaining rods are one corner rod and eight interior rods.

Table 4 Flow Areas and Diameters for Target Rods

Parameter	[redacted]	50 µm gap (6.100 mm OD)	[redacted]
Corner Rod			
Flow Area	[redacted]	133.29 mm^2 (0.20660 in^2)	[redacted]
Hydraulic Diameter		9.55 mm 0.3760 in)	
Heated Diameter		27.82 mm (1.0953 in)	
Interior Rod			
Flow Area	[redacted]	123.31 mm^2 (0.19112 in^2)	[redacted]
Hydraulic Diameter		10.74 mm (0.4228 in)	
Heated Diameter		25.74 mm (1.0134 in)	

5a, b, f

[redacted]

Table 4 Flow Areas and Diameters for Target Rods

Parameter	[redacted]	50 µm gap (6.100 mm OD)	[redacted]
Eight Interior Rods and One Corner Rod			
Flow Area	Only Nominal Used	1119.70 mm^2 (1.73554 in2)	Only Nominal Used
Hydraulic Diameter		10.58 mm (0.4165 in)	
Heated Diameter		25.97 mm (1.0224 in.)	
Seven Interior Rods and Two Corner Rods			
Flow Area	Only Nominal Used	1129.70 mm^2 (1.75104 in2)	Only Nominal Used
Hydraulic Diameter		10.44 mm (0.4110 in)	
Heated Diameter		26.20 mm (1.0315 in)	

5a, b, f

5.2 Target Steady State Power Distribution

Steady state power distributions are based on detailed MCNP6 analyses (30441R00031). MCNP6 produced results for each target rod in both target assemblies using 25 axial nodes. The input for RELAP5 uses 20 axial nodes to represent the stack of 100 target pellets. The MCNP6 results were averaged in a piece-wise fashion to generate 20 data points. The RELAP5 model explicitly analyzes rods 5 and 6 in target assembly 1 and rods 17 and 22 in target assembly 2. The remaining rods in each target assembly are averaged together in the RELAP5 model. The rods with the peak power density (5 and 17) are obtained from the Extreme MCNP6 case 30 (30441R00031). The peak power density case has more control blade insertion which makes the power density more peaked below the core mid-plane. The other rods modeled in RELAP5 are based on the Maximum MCNP6 case 44 with less control blade insertion which maximizes both rod and assembly power. Rod 17 has the peak power density and is analyzed in RELAP5, FRAPCON, and FRAPTRAN. The FRAPCON and FRAPTRAN input needs 21 data points at the mesh lines of the 20 axial nodes. Figure 4 through Figure 9 presents the axial power factors generated by MCNP6 along with the factors used in RELAP5. Figure 7 also includes the axial power factors used in FRAPCON and FRAPTRAN for target rod 17 and Figure 8 includes axial power factors used for FRAPTRAN analysis for target rod 22.

[redacted]

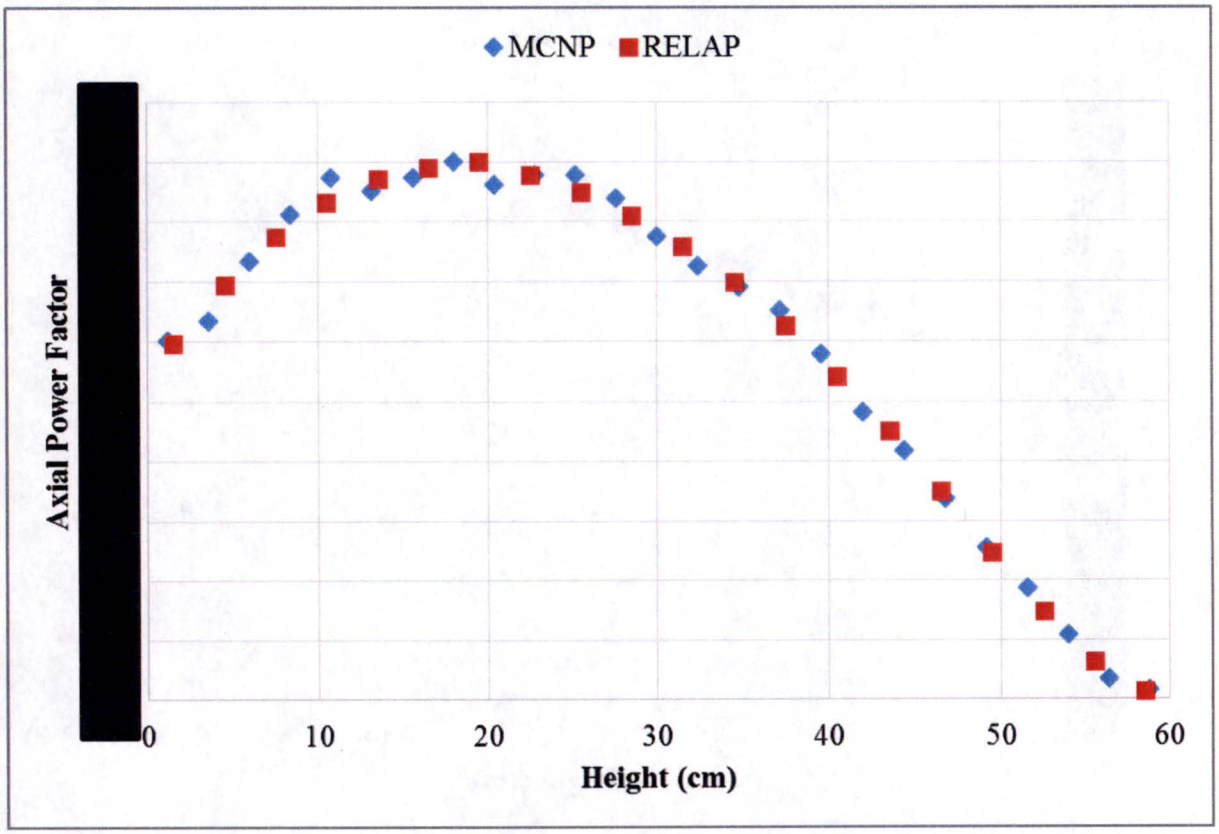

5a, d, e, f

Figure 4. Axial power factor for target rod 5

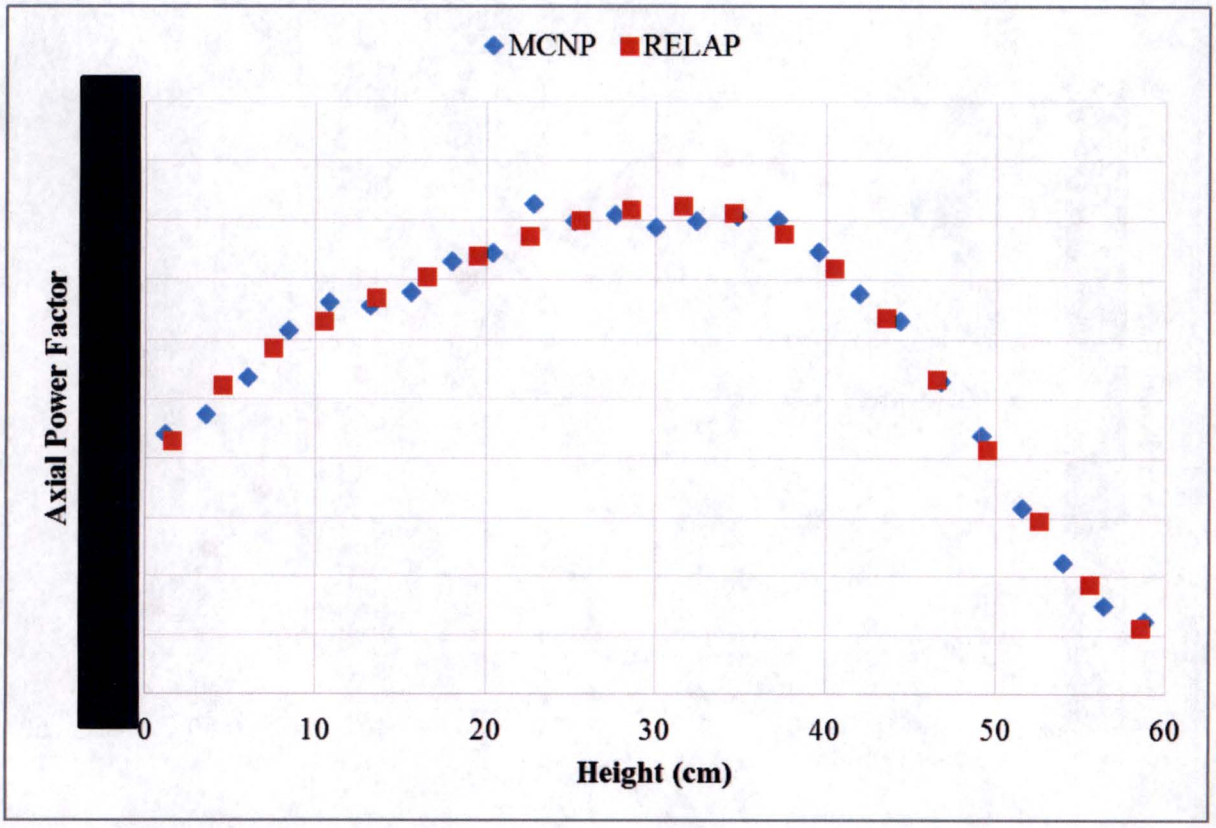

5a, d, e, f

Figure 5. Axial power factors for target rod 6

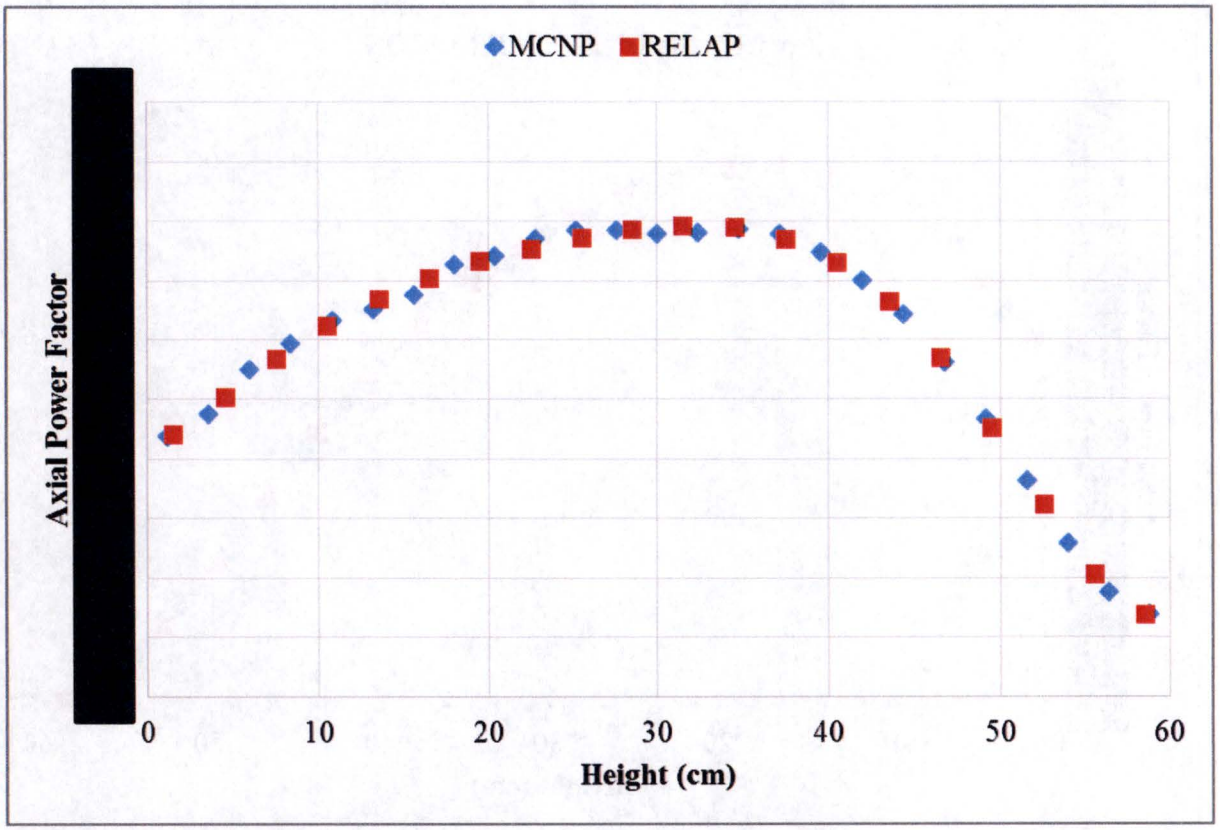

5a, d, e, f

Figure 6. Axial power factors for target rods 1 thru 4 and 7 thru 11

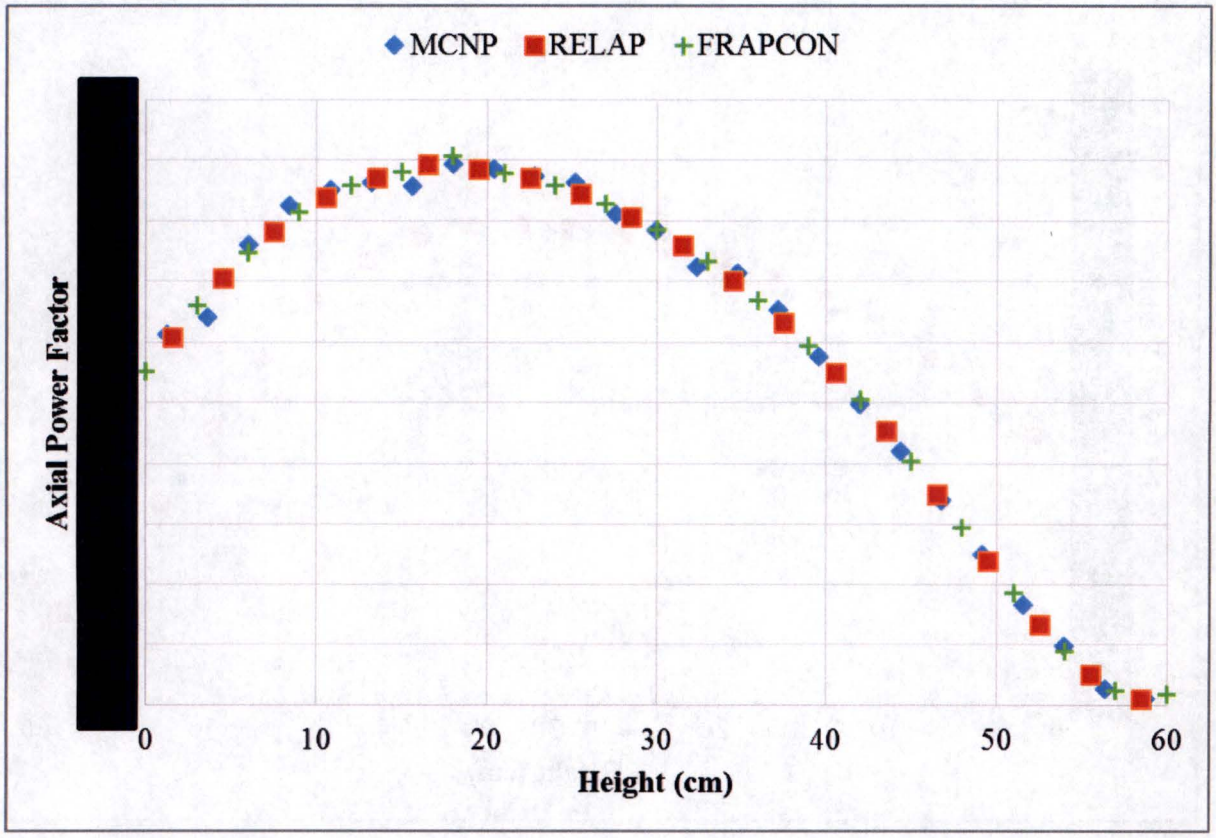

5a, d, e, f

Figure 7. Axial power factors for target rod 17

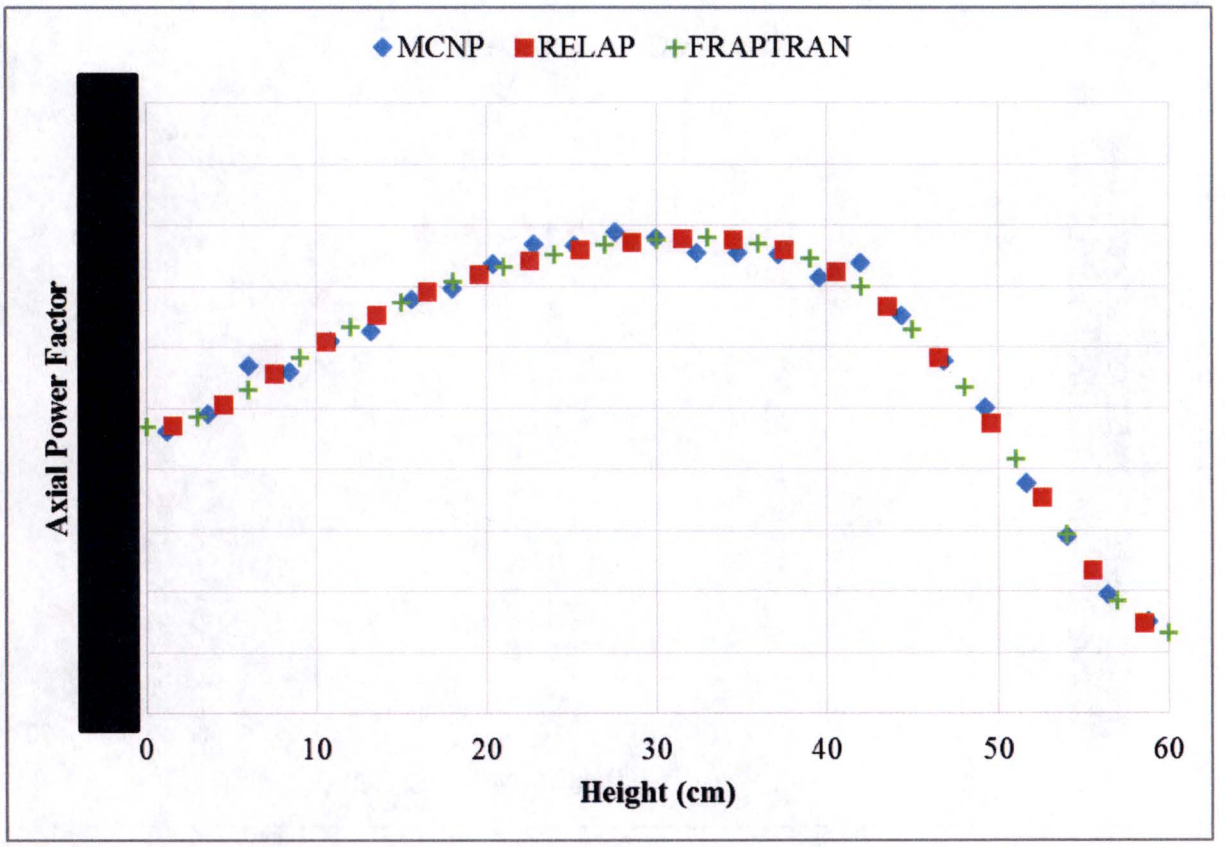

5a, d, e, f

Figure 8. Axial power factors for target rod 22

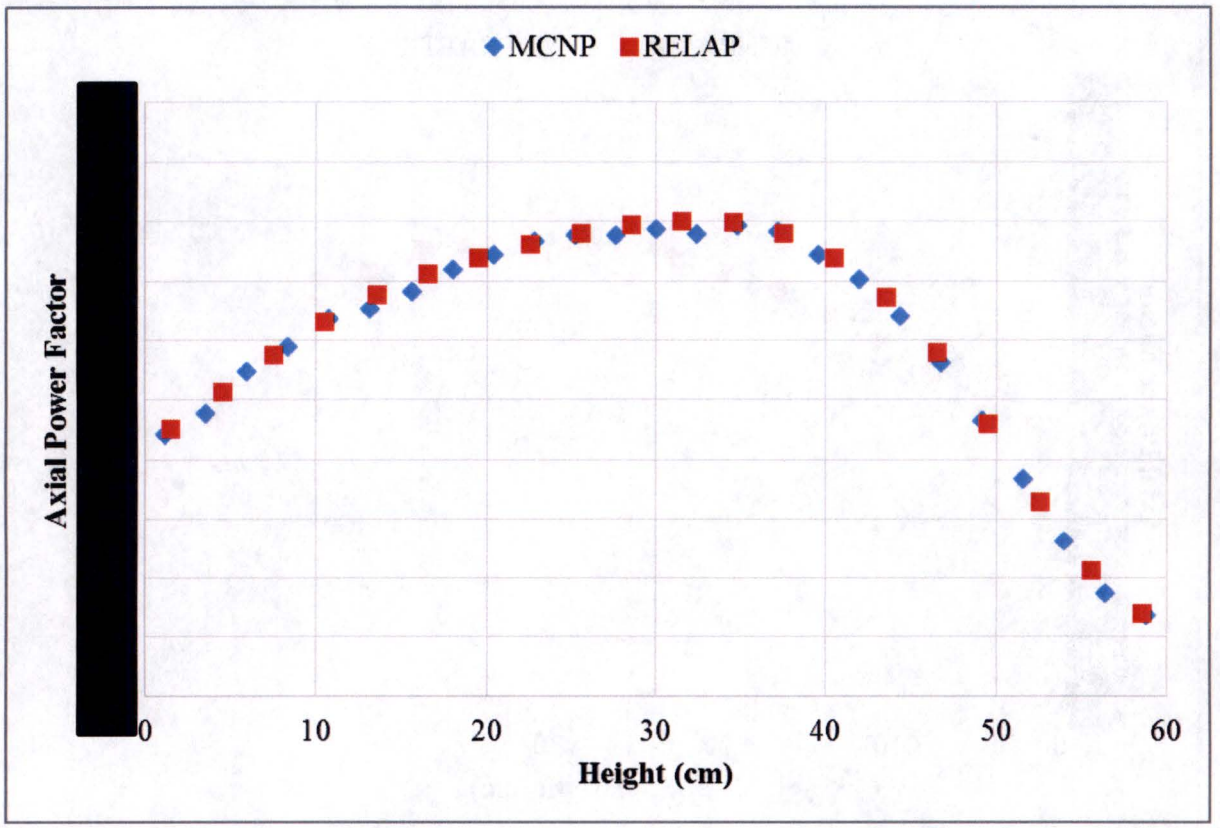

5a, d, e, f

Figure 9. Axial power factors for target rods 12 thru 16 and 18 thru 21

The total target rod powers are presented in Table 5 and conservatively include 2-sigma uncertainties from statistical error, density, enrichment, and target rod position (30441R00031). Target rods 5 and 17 have uncertainties of [redacted] Target rods 6 and 22 have uncertainties of [redacted] All of the remaining rods represent have an uncertainty of [redacted] based on the total target power. The target rod power for the average rods 1-4, 7-11, 11-16, and 18-21 are based on the nominal 50 μm (1.97 mil) gap pellet volume.

5a, d, e, f

Table 5 Target Rod Power

Target Rods	Power per rod
Rod 5	
Rod 6	
Rod 1-4, 7-11 (Average)	
Rod 17	
Rod 22	
Rods 11-16, 18-21 (Average)	

5a, d, e, f

[redacted]

FRAPCON and FRAPTRAN power input for target rod 17 uses the RELAP5 value divided by the pellet stack height of 0.6 m and converted to units of kW/m. This value is then modified by an axial power factor to get the linear power at a given height.

5.3 RELAP5 Hydrodynamic Components

The steady state RELAP5 model of the target cooling system (Figure 1) does not include the target DHRS valves. The steady state model also does not include the target cooling system pump or heat exchanger. The steady state RELAP5 model uses time dependent volumes and time dependent junctions to replace the pump and heat exchanger.

The RELAP5 models for the loss of coolant accident (LOCA) and loss of pump flow (LOPF) accident are essentially the same except for the trip logic and the addition of break valves to the LOCA model. The volume data for the hydrodynamic components in the RELAP5 model are presented in Table 6. Volume 80 has a flow area expander so 3 different areas are used. Volume 102 has a flow area reducer in that pipe so 3 different areas are used. Other volumes in the target assembly also have area changes associated with their flow paths.

Table 6 RELAP5 Volumes

Description	Volume ID	Area (m^2)	Length (m)	Angle (°)	Roughness (m)
Pump	075-01	4.769-3	0.1382	90.0	
Pump outlet to HX inlet	080-01	4.769-3	0.986	90.0	1.9-6
	080-02	4.769-3	0.410	0.0	1.9-6
	080-03	4.769-3	0.225	0.0	1.9-6
	080-04	6.376-3	0.990	0.0	1.6-6
	080-05	8.213-3	1.340	0.0	1.3-6
Heat exchanger (HX)	090-01	0.0163	0.254	-31.79	1.4-3
	090-02	0.0163	0.254	-31.79	1.4-3
	090-03	0.0163	0.254	-31.79	1.4-3
	090-04	0.0163	0.254	-31.79	1.4-3
	090-05	0.0163	0.254	-31.79	1.4-3
	090-06	0.0163	0.254	-31.79	1.4-3
	090-07	0.0163	0.254	-31.79	1.4-3
	090-08	0.0163	0.254	-31.79	1.4-3
	090-09	0.0163	0.254	-31.79	1.4-3
	090-10	0.0163	0.254	-31.79	1.4-3
HX outlet to wye	100-01	8.213-3	0.733	0.0	1.3-6
	100-02	8.213-3	0.612	0.0	1.3-6
	100-03	8.213-3	1.485	0.0	1.3-6
	100-04	8.213-3	1.181	0.0	1.3-6
	100-05	8.213-3	0.225	0.0	1.3-6
	100-06	8.213-3	0.842	10.95	1.3-6

Table 6 RELAP5 Volumes

Description	Volume ID	Area (m^2)	Length (m)	Angle (°)	Roughness (m)
	100-07	8.213-3	0.150	0.0	1.3-6
Wye to isolation valve	102-01	8.213-3	0.308	0.0	1.3-6
	102-02	8.213-3	0.138	0.0	1.3-6
	102-03	6.376-3	0.244	0.0	1.6-6
	102-04	4.769-3	0.549	0.0	1.9-6
	102-05	4.769-3	0.479	0.0	1.9-6
	102-06	4.769-3	0.673	0.0	1.9-6
Isolation valve to natural	104-01	4.769-3	0.418	0.0	1.9-6
circulation valve tee	104-02	4.769-3	0.305	0.0	1.9-6
	104-03	4.769-3	0.230	0.0	1.9-6
	104-04	4.769-3	0.230	0.0	1.9-6
	104-05	4.769-3	0.305	0.0	1.9-6
	104-06	4.769-3	1.380	0.0	1.9-6
	104-07	4.769-3	1.108	0.0	1.9-6
	104-08	4.769-3	1.032	0.0	1.9-6
	104-09	4.769-3	0.230	-90.0	1.9-6
	104-10	4.769-3	0.573	-90.0	1.9-6
	104-11	4.769-3	0.573	-90.0	1.9-6
	104-12	4.769-3	0.077	-90.0	1.9-6
From tee to nat. circ. valve	106-01	2.027-3	0.170	0.0	1.9-6
From tee to tee	108-01	4.769-3	0.077	-90.0	1.9-6
	108-02	4.769-3	0.077	-90.0	1.9-6
From tee to nat. circ. valve	110-01	2.027-3	0.170	0.0	1.9-6
Natural circulation valve tee to	112-01	4.769-3	1.000	-90.0	1.9-6
TA	112-02	4.769-3	1.000	-90.0	1.9-6
	112-03	4.769-3	0.872	-90.0	1.9-6
	112-04	4.769-3	0.406	0.0	1.9-6
	112-05	4.769-3	0.508	-90.0	1.9-6
	112-06	4.769-3	0.406	0.0	1.9-6
	112-07	4.769-3	0.770	-90.0	1.9-6
	112-08	4.769-3	0.865	-90.0	1.9-6
	112-09	4.769-3	0.305	-90.0	1.9-6
	112-10	4.769-3	0.443	-90.0	1.9-6
TA top to lower plenum	114-01	1.795-2	0.091	-90.0	5.0-5
	114-02	2.806-2	0.613	-90.0	5.0-5
	114-03	1.694-2	0.106	-90.0	5.0-5
Lower plenum	115-01	9.677-3	0.152	0.0	3.0-5
From lower plenum to target	116-01	3.401-3	0.045	90.0	1.6-6
rod holder	116-02	1.937-3	6.30-3	90.0	1.6-6
Target rod holder	117-01	1.044-3	9.18-3	0.0	1.5-5
Target rods 1-4, 7-11	121-01	1.1297-3	0.030	90.0	1.0-6
	121-02	1.1297-3	0.030	90.0	1.0-6
	121-03	1.1297-3	0.030	90.0	1.0-6
	121-04	1.1297-3	0.030	90.0	1.0-6

[redacted]

Table 6 RELAP5 Volumes

Description	Volume ID	Area (m^2)	Length (m)	Angle (°)	Roughness (m)
	121-05	1.1297-3	0.030	90.0	1.0-6
	121-06	1.1297-3	0.030	90.0	1.0-6
	121-07	1.1297-3	0.030	90.0	1.0-6
	121-08	1.1297-3	0.030	90.0	1.0-6
	121-09	1.1297-3	0.030	90.0	1.0-6
	121-10	1.1297-3	0.030	90.0	1.0-6
	121-11	1.1297-3	0.030	90.0	1.0-6
	121-12	1.1297-3	0.030	90.0	1.0-6
	121-13	1.1297-3	0.030	90.0	1.0-6
	121-14	1.1297-3	0.030	90.0	1.0-6
	121-15	1.1297-3	0.030	90.0	1.0-6
	121-16	1.1297-3	0.030	90.0	1.0-6
	121-17	1.1297-3	0.030	90.0	1.0-6
	121-18	1.1297-3	0.030	90.0	1.0-6
	121-19	1.1297-3	0.030	90.0	1.0-6
	121-20	1.1297-3	0.030	90.0	1.0-6
	121-21	1.1297-3	0.0457	90.0	1.0-6
Target rod 6	122-01	1.2057-4	0.030	90.0	1.0-6
	122-02	1.2057-4	0.030	90.0	1.0-6
	122-03	1.2057-4	0.030	90.0	1.0-6
	122-04	1.2057-4	0.030	90.0	1.0-6
	122-05	1.2057-4	0.030	90.0	1.0-6
	122-06	1.2057-4	0.030	90.0	1.0-6
	122-07	1.2057-4	0.030	90.0	1.0-6
	122-08	1.2057-4	0.030	90.0	1.0-6
	122-09	1.2057-4	0.030	90.0	1.0-6
	122-10	1.2057-4	0.030	90.0	1.0-6
	122-11	1.2057-4	0.030	90.0	1.0-6
	122-12	1.2057-4	0.030	90.0	1.0-6
	122-13	1.2057-4	0.030	90.0	1.0-6
	122-14	1.2057-4	0.030	90.0	1.0-6
	122-15	1.2057-4	0.030	90.0	1.0-6
	122-16	1.2057-4	0.030	90.0	1.0-6
	122-17	1.2057-4	0.030	90.0	1.0-6
	122-18	1.2057-4	0.030	90.0	1.0-6
	122-19	1.2057-4	0.030	90.0	1.0-6
	122-20	1.2057-4	0.030	90.0	1.0-6
	122-21	1.2057-4	0.0457	90.0	1.0-6
Target rod 5	123-01	1.2057-4	0.030	90.0	1.0-6
	123-02	1.2057-4	0.030	90.0	1.0-6
	123-03	1.2057-4	0.030	90.0	1.0-6
	123-04	1.2057-4	0.030	90.0	1.0-6
	123-05	1.2057-4	0.030	90.0	1.0-6
	123-06	1.2057-4	0.030	90.0	1.0-6

Table 6 RELAP5 Volumes

Description	Volume ID	Area (m^2)	Length (m)	Angle (°)	Roughness (m)
	123-07	1.2057-4	0.030	90.0	1.0-6
	123-08	1.2057-4	0.030	90.0	1.0-6
	123-09	1.2057-4	0.030	90.0	1.0-6
	123-10	1.2057-4	0.030	90.0	1.0-6
	123-11	1.2057-4	0.030	90.0	1.0-6
	123-12	1.2057-4	0.030	90.0	1.0-6
	123-13	1.2057-4	0.030	90.0	1.0-6
	123-14	1.2057-4	0.030	90.0	1.0-6
	123-15	1.2057-4	0.030	90.0	1.0-6
	123-16	1.2057-4	0.030	90.0	1.0-6
	123-17	1.2057-4	0.030	90.0	1.0-6
	123-18	1.2057-4	0.030	90.0	1.0-6
	123-19	1.2057-4	0.030	0.0	1.0-6
	123-20	1.2057-4	0.030	90.0	1.0-6
	123-21	1.2057-4	0.0457	90.0	1.0-6
Upper target rod positioner	125-01	1.2265-3	6.35-3	0.0	1.5-6
Target hold-down and diffuser	135-01	1.9426-3	0.018	90.0	1.6-6
	135-02	6.208-3	0.027	90.0	1.6-6
	135-03	1.9968-3	0.1182	90.0	1.6-6
	135-04	2.0258-3	0.0528	90.0	1.6-6
	135-05	2.0258-3	0.0528	0.0	1.6-6
Pool inlet to pump inlet	302-01	4.769-3	0.689	90.0	1.9-6
	302-02	4.769-3	0.689	90.0	1.9-6
	302-03	4.769-3	0.689	90.0	1.9-6
	302-04	4.769-3	0.689	90.0	1.9-6
	302-05	4.769-3	0.230	90.0	1.9-6
	302-06	4.769-3	1.019	0.0	1.9-6
	302-07	4.769-3	1.066	0.0	1.9-6
	302-08	4.769-3	0.920	0.0	1.9-6
	302-09	4.769-3	0.936	0.0	1.9-6
	302-10	4.769-3	1.437	0.0	1.9-6
	302-11	4.769-3	0.305	0.0	1.9-6
	302-12	4.769-3	0.230	0.0	1.9-6
	302-13	4.769-3	0.230	0.0	1.9-6
	302-14	4.769-3	0.305	0.0	1.9-6
	302-15	4.769-3	0.196	0.0	1.9-6
	302-16	4.769-3	1.167	0.0	1.9-6
	302-17	4.769-3	1.167	0.0	1.9-6
	302-18	4.769-3	0.413	0.0	1.9-6
	302-19	4.769-3	0.354	0.0	1.9-6
	302-20	4.769-3	0.309	10.06	1.9-6
	302-21	4.769-3	1.079	0.0	1.9-6
	302-22	4.769-3	0.664	0.0	1.9-6
	302-23	4.769-3	0.407	0.0	1.9-6

Table 6 RELAP5 Volumes

Description	Volume ID	Area (m^2)	Length (m)	Angle (°)	Roughness (m)
	302-24	4.769-3	0.483	0.0	1.9-6
Reactor pool	500-01	7.0686	10.00	-90.0	1.0-3
	500-02	7.0686	0.893	-90.0	1.0-3
	500-03	7.0686	0.154	-90.0	1.0-3
	500-04	7.0686	0.154	-90.0	1.0-3
	500-05	7.0686	0.154	-90.0	1.0-3
	500-06	7.0686	1.225	-90.0	1.0-3
	500-07	7.0686	3.941	-90.0	1.0-3
	500-08	7.0686	0.340	-90.0	1.0-3
	500-09	7.0686	0.103	-90.0	1.0-3
Secondary side HX inlet	400-01	1.0	1.0	0.0	0.0
Secondary side HX	406-01	0.0163	0.254	31.79	1.3-3
	406-02	0.0163	0.254	31.79	1.3-3
	406-03	0.0163	0.254	31.79	1.3-3
	406-04	0.0163	0.254	31.79	1.3-3
	406-05	0.0163	0.254	31.79	1.3-3
	406-06	0.0163	0.254	31.79	1.3-3
	406-07	0.0163	0.254	31.79	1.3-3
	406-08	0.0163	0.254	31.79	1.3-3
	406-09	0.0163	0.254	31.79	1.3-3
	406-10	0.0163	0.254	31.79	1.3-3
Secondary side HX outlet	408-01	1.0	1.0	0.0	0.0

Hydrodynamic components 102 through 136 are duplicated for components 202 through 236 to model flow through the second target assembly. The only difference is in the flow areas in the target assembly volumes 221, 222, and 223 (per Table 4). The junction data for hydrodynamic components with non-zero K-loss factors are presented in Table 7.

Table 7 RELAP5 Junctions with Non-Zero K-Loss Factors

Description	Junction ID	Area (m^2)	K Loss forward	K Loss reverse
Pump inlet	75-01	4.769-3	0.04	0.04
Pump outlet	75-02	4.769-3	0.04	0.04
Pump outlet to HX inlet	80-01	4.769-3	0.111	0.111
	80-02	4.769-3	0.200	0.200
	80-03	4.769-3	0.187	0.187
HX inlet	85-00	8.213-3	0.500	0.500
Heat exchanger (HX)	90-01	0.0163	7.0	7.0
	90-02	0.0163	7.0	7.0
	90-03	0.0163	7.0	7.0

[redacted]

Table 7 RELAP5 Junctions with Non-Zero K-Loss Factors

Description	Junction ID	Area (m^2)	K Loss forward	K Loss reverse
	90-04	0.0163	7.0	7.0
	90-05	0.0163	7.0	7.0
	90-06	0.0163	7.0	7.0
	90-07	0.0163	7.0	7.0
	90-08	0.0163	7.0	7.0
	90-09	0.0163	7.0	7.0
HX outlet	95-00	8.213-3	0.500	0.500
HX outlet to wye	100-01	8.213-3	0.097	0.097
	100-02	8.213-3	1.000	1.000
	100-03	8.213-3	0.050	0.050
	100-04	8.213-3	0.097	0.097
	100-05	8.213-3	0.650	0.650
	100-06	8.213-3	0.650	0.650
Wye to TA 1	101-01	8.213-3	0.100	0.100
Wye to TA 2	101-02	8.213-3	0.100	0.100
Wye to Isolation valve	102-01	8.213-3	0.050	0.050
	102-02	8.213-3	0.187	0.187
Isolation valve	103-00	4.769-3	0.400	0.400
Isolation valve to natural	104-01	4.769-3	0.750	0.750
circulation valve tee	104-02	4.769-3	0.750	0.750
	104-03	4.769-3	0.116	0.116
	104-04	4.769-3	0.750	0.750
	104-05	4.769-3	0.750	0.750
	104-06	4.769-3	0.116	0.116
	104-07	4.769-3	0.020	0.020
	104-08	4.769-3	0.116	0.116
From tee to nat. circ. valve	105-0101	4.769-3	0.200	0.200
	105-0102	2.027-3	0.800	0.800
Natural circulation valve	107-00	2.027-3	1.600	1.100
From tee to nat. circ. valve	109-0101	4.769-3	0.200	0.200
	109-0102	2.027-3	0.800	0.800
From natural circulation valve tee	112-03	4.769-3	0.116	0.116
to TA	112-04	4.769-3	0.116	0.116
	112-05	4.769-3	0.116	0.116
	112-06	4.769-3	0.116	0.116
	112-08	4.769-3	0.750	0.750
	112-09	4.769-3	0.750	0.750
Target assembly (TA) inlet	113-00	4.769-3	0.500	0.500
TA top to lower plenum	114-01	1.795-2	2.73	2.73
	114-02	1.694-2	2.73	2.73
Lower plenum	115-01	9.677-3	2.50	2.50
	115-02	3.401-3	0.400	0.400
After lower plenum	116-01	1.937-3	0.400	0.400

Table 7 RELAP5 Junctions with Non-Zero K-Loss Factors

Description	Junction ID	Area (m^2)	K Loss forward	K Loss reverse
Target rod holder inlet	117-01	1.044-3	0.300	0.300
Inlet to target rods 1-4, 7-11	117-02	1.1297-3	0.300	0.300
Inlet to target rod 6	117-03	1.2057-4	0.300	0.300
Inlet to target rod 5	117-04	1.2057-4	0.300	0.300
Exit from target rods 1-4, 7-11	125-01	1.1297-3	1.60	1.60
Exit from target rod 6	125-02	1.2057-4	1.60	1.60
Exit from target rod 5	125-03	1.2057-4	1.60	1.60
Upper target rod positioner	125-04	1.9426-3	2.10	2.10
Target hold-down and diffuser	135-01	1.9426-3	0.600	0.600
	135-02	1.9968-3	0.250	0.250
	135-03	1.9968-3	0.550	0.550
	135-04	2.0258-3	1.25	1.25
Diffuser exit to pool	136-00	2.0258-3	1.00	0.500
Pool inlet to cooling water	301-00	4.769-3	0.500	0.500
Pool inlet to pump inlet	302-05	4.769-3	0.116	0.116
	302-06	4.769-3	0.116	0.116
	302-08	4.769-3	0.040	0.040
	302-09	8.213-3	0.116	0.116
	302-10	4.769-3	0.560	0.560
	302-11	4.769-3	0.560	0.560
	302-12	4.769-3	0.116	0.116
	302-13	4.769-3	0.560	0.560
	302-14	4.769-3	0.560	0.560
	302-17	4.769-3	0.560	0.560
	302-18	4.769-3	0.560	0.560
	302-20	4.769-3	0.116	0.116
	302-21	4.769-3	1.000	1.000
	302-22	4.769-3	0.116	0.116
	302-23	4.769-3	0.050	0.050
Pool water / air surface	500-01	7.0686	5.00	5.00
Secondary side HX	406-01	0.0163	6.00	6.00
	406-02	0.0163	6.00	6.00
	406-03	0.0163	6.00	6.00
	406-04	0.0163	6.00	6.00
	406-05	0.0163	6.00	6.00
	406-06	0.0163	6.00	6.00
	406-07	0.0163	6.00	6.00
	406-08	0.0163	6.00	6.00
	406-09	0.0163	6.00	6.00

5.4 RELAP5 Pump Model

RELAP5 includes pump curves for two different models of pump. Because the exact model and associated performance data for the target cooling system pump remains to be specified by the supplier of the cooling system skid, the Westinghouse pump was selected with input data appropriate for this application. The pump head and velocity are adjusted in the RELAP5 model to match the flow rate through the target assembly. K-loss factors within the target assembly are also adjusted to match the pressures predicted by FLUENT (30441R00038). The pump parameters in Table 8 produce the desired characteristics but would be updated as the pump design is finalized and cooling system pressure drops are verified.

Table 8 RELAP5 Pump Parameters

Parameter	Value
Rated pump speed	185 rad/s (1770 rpm)
Pump speed ratio	0.9069
Rated pump flow	0.01351 m^3/s (214 gpm)
Rated pump head	31.1 m (102 ft)
Rated pump torque	54.37 N-m (40.10 lb-ft)
Pump moment of inertia	0.0603 kg/m^2 (14.3 lb/ft^2)

5.5 RELAP5 Heat Exchanger Model

A plate heat exchanger will likely be selected by the subcontractor supplying the target cooling system skid and its performance will meet the specified requirements. The RELAP5 model can approximate a plate heat exchanger and the parameters in Table 9 closely match the expected inlet and outlet conditions at the design flow rate.

Table 9 RELAP5 Heat Exchanger Parameters

Parameter	Value
Primary inlet temperature	322.12 K (48.97 °C)
Primary outlet temperature	311.98 K (38.83 °C)
Secondary inlet temperature	302.0 K 28.85 °C)
Secondary outlet temperature	313.6 K (40.45 °C)
Primary inlet pressure	0.2556 MPa
Primary outlet pressure	0.1981 MPa
Secondary inlet pressure	0.3546 MPa
Secondary outlet pressure	0.2839 MPa
Primary flow rate	13.46 kg/s
Secondary flow rate	13.00 kg/s
Flow area	0.0163 m^2
Heat transfer area	2.175 m^2
Height	1.70 m
Flow gap	2 mm
Flow length	2.54 m
Plate thickness	1 mm
Surface roughness	0.0014 m
K-loss per turn (10 turns)	7.0

5.6 Steady State Inputs from RELAP

Steady state RELAP5 runs were performed for the [redacted] gap and [redacted] gap cases at nominal (100%) flow of [redacted] through the target assembly at 100% and 115% reactor and target power. Steady state RELAP5 runs were also performed at 85% flow for the [redacted] gap and [redacted] gap cases at 100% power and 115% power. RELAP5 cladding surface temperatures at the node centers for target rod 17 were averaged or extrapolated to produce the mesh line temperatures required by FRAPCON. Table 10 through Table 12 present the RELAP5 results and FRAPCON input values in Kelvin. RELAP5 coolant pressures along target rod 17 are presented in Table 13. The mass flux in the flow channel around target rod 17 is presented in Table 14.

5a, b, d, e, f

[redacted]

Table 10 Cladding Surface Temperature at 100% Power and 100% Flow in Kelvin

5a, b, f

[redacted] gap		[redacted] gap	
RELAP Result	FRAPCON Input	RELAP Result	FRAPCON Input
427.22	425.09	426.66	424.50
433.11	430.06	432.54	429.50
437.21	434.95	436.65	434.40
439.90	438.79	439.34	438.23
441.47	441.23	440.91	440.67
442.47	442.33	441.91	441.76
442.06	442.36	441.50	441.79
441.37	441.65	440.81	441.08
440.13	440.47	439.56	439.91
438.33	438.97	437.77	438.41
435.94	437.11	435.38	436.56
432.81	434.70	432.25	434.14
428.75	431.37	428.20	430.81
423.48	426.71	422.93	426.14
416.62	420.31	416.06	419.74
407.71	411.95	407.15	411.38
396.39	401.75	395.81	401.20
384.29	390.43	383.81	389.91
374.64	379.50	374.25	379.04
370.20	371.60	369.84	371.22
	370.83		370.54

Table 11 Cladding Surface Temperature at 115% Power and 100% Flow in Kelvin

5a, b, f

[redacted] gap		[redacted] gap	
RELAP Result	FRAPCON Input	RELAP Result	FRAPCON Input
436.01	434.25	435.45	433.69
441.57	438.65	441.01	438.09
445.50	443.26	444.93	442.70
448.09	447.00	447.53	446.43
449.62	449.42	449.05	448.85
450.60	450.53	450.03	449.96
450.22	450.56	449.65	449.99
449.57	449.84	448.99	449.27
448.37	448.66	447.80	448.08
446.65	447.17	446.08	446.60
444.35	445.39	443.78	444.82
441.34	443.11	440.78	442.55
437.45	440.00	436.90	439.44
432.42	435.64	431.86	435.07
425.89	429.59	425.34	429.02
417.48	421.58	416.93	421.02
406.86	411.65	406.31	411.09
394.28	400.38	393.74	399.83
383.31	389.11	382.86	388.59
378.25	380.24	377.84	379.77
	377.56		377.19

[redacted]

Table 12 Cladding Surface Temperature at 115% Power and 85% Flow in Kelvin

5a, b, f

[redacted] gap		[redacted] gap	
RELAP Result	FRAPCON Input	RELAP Result	FRAPCON Input
439.30	437.74	438.79	437.25
444.11	441.59	443.60	441.07
447.55	445.60	447.03	445.08
449.85	448.86	449.33	448.34
451.22	451.01	450.69	450.49
452.12	452.03	451.59	451.50
451.82	452.11	451.29	451.59
451.28	451.53	450.75	451.00
450.27	450.53	449.74	450.00
448.79	449.24	448.27	448.71
446.81	447.68	446.28	447.15
444.21	445.69	443.69	445.17
440.85	443.01	440.34	442.50
436.50	439.28	436.00	438.78
430.90	434.13	430.40	433.64
423.70	427.30	423.20	426.80
414.61	418.75	414.12	418.25
403.71	408.83	403.21	408.33
392.57	398.51	392.07	398.02
386.90	389.55	386.45	389.07
	384.78		384.36

Table 13 Target Rod 17 Coolant Pressure in Pascals

100% Power 100% Flow		115% Power 100% Flow		115% Power 85% Flow	
[redacted] gap	[redacted] gap	[redacted] gap	[redacted] gap	[redacted] gap	[redacted] gap
2.32310E+05	2.32390E+05	2.32311E+05	2.32392E+05	2.17050E+05	2.17109E+05
2.31326E+05	2.31402E+05	2.31327E+05	2.31403E+05	2.16241E+05	2.16297E+05
2.30343E+05	2.30414E+05	2.30343E+05	2.30415E+05	2.15433E+05	2.15485E+05
2.29361E+05	2.29428E+05	2.29361E+05	2.29429E+05	2.14626E+05	2.14675E+05
2.28380E+05	2.28443E+05	2.28381E+05	2.28444E+05	2.13821E+05	2.13866E+05
2.27401E+05	2.27459E+05	2.27401E+05	2.27460E+05	2.13016E+05	2.13059E+05
2.26423E+05	2.26477E+05	2.26424E+05	2.26478E+05	2.12214E+05	2.12253E+05
2.25447E+05	2.25496E+05	2.25448E+05	2.25498E+05	2.11412E+05	2.11448E+05
2.24472E+05	2.24517E+05	2.24473E+05	2.24519E+05	2.10612E+05	2.10645E+05
2.23498E+05	2.23539E+05	2.23501E+05	2.23542E+05	2.09814E+05	2.09844E+05
2.22526E+05	2.22563E+05	2.22530E+05	2.22567E+05	2.09017E+05	2.09044E+05
2.21556E+05	2.21588E+05	2.21560E+05	2.21593E+05	2.08222E+05	2.08245E+05
2.20586E+05	2.20614E+05	2.20592E+05	2.20621E+05	2.07428E+05	2.07448E+05
2.19619E+05	2.19642E+05	2.19626E+05	2.19651E+05	2.06635E+05	2.06652E+05
2.18653E+05	2.18672E+05	2.18662E+05	2.18682E+05	2.05844E+05	2.05858E+05
2.17688E+05	2.17703E+05	2.17699E+05	2.17715E+05	2.05054E+05	2.05065E+05
2.16724E+05	2.16735E+05	2.16737E+05	2.16749E+05	2.04266E+05	2.04274E+05
2.15762E+05	2.15768E+05	2.15777E+05	2.15785E+05	2.03479E+05	2.03483E+05
2.14800E+05	2.14803E+05	2.14818E+05	2.14822E+05	2.02693E+05	2.02694E+05
2.13840E+05	2.13838E+05	2.13861E+05	2.13859E+05	2.01907E+05	2.01906E+05
2.12630E+05	2.12623E+05	2.12654E+05	2.12648E+05	2.00918E+05	2.00913E+05

5a, b, f

Table 14 Target Rod 17 Mass Flux

100% Power 100% Flow		115% Power 100% Flow		115% Power 85% Flow	
[redacted] gap	[redacted] gap	[redacted] gap	[redacted] gap	[redacted] gap	[redacted] gap
[redacted]	[redacted]	[redacted]	[redacted]	[redacted]	[redacted]

5a, b, d, e, f

5.7 Reactivity Transient Power History

The MURR reactivity transient for a 600 per cent mille (pcm) rapid reactivity insertion is described in the MURR SAR for relicensing and summarized below in Section 6.1. MURR provided General Atomics (GA) with an EXCEL file containing the power prediction for this transient. It was manipulated within the EXCEL file to provide the data in the format needed by FRAPTRAN.

The MURR reactivity transient for a 30 pcm per second control blade withdrawal is also described in the MURR SAR for relicensing and summarized below in Section 6.2. The slow reactivity addition coupled with negative temperature feedback produces a gradual power ramp which was added to the MURR EXCEL spreadsheet and manipulated to provide the data in the format needed by FRAPTRAN.

[redacted]

6 RESULTS AND CONCLUSIONS

6.1 Rapid Insertion of Positive Reactivity

For the Insertion of Excess Reactivity accident analysis, the licensed maximum power level of 10 MW was used in the reactor SAR as the starting assumption since MURR does not, nor can it legally, operate above this power level. NUREG-1537, Part 2, page 13-9, Standard Review Plan and Acceptance Criteria, states for Insertion of Excess Reactivity accident, that "The accident scenario assumes that the reactor has a maximum load of fuel (consistent with the technical specifications), the reactor is operating at full licensed power, and the control system..." The accident was re-analyzed at a much more conservative starting power level (11.5 MW) than is required by NUREG-1537 and the results are provided below. 11.5 MW was chosen, instead of the Limiting Safety System Setting (LSSS) set point of 12.5 MW, since the rod run-in system will initiate a rod run-in at 11.5 MW (Technical Specification 3.2.f.1) and shutdown the reactor prior to reaching the LSSS SCRAM set point of 125%.

For the reactor SAR analysis of the Insertion of Excess Reactivity accident, the temperature coefficient used was -6.0×10^{-5} **Δk/k and not** -7.0×10^{-5} **Δk/k as stated in the previous version of** the reactor SAR. The third paragraph on Page 13-17 of the SAR lists the various reactivity coefficients assumed for the Insertion of Excess Reactivity accident analysis.

For both the reactor SAR analyses, as well as for the updated analysis presented here, the control blade insertion times are based on the current and relicensing Technical Specification 3.2.c requirement of insertion to the 20% withdrawn position in less than 0.7 seconds. So the insertion rate was calculated based on shim control blades travelling from 26 inches (fully withdrawn) to 5.2 inches (20% withdrawn or 80% inserted) in 0.7 seconds. This is a conservative assumption since monthly control blade drop time verifications performed at MURR have always yielded insertion times of 0.6 seconds or less.

Similar to the reactor SAR analysis, the Reactivity Transient Analysis program PARET (V7.5), maintained and distributed by the Nuclear Engineering Division of Argonne National Laboratory (ANL) was used. For the Insertion of Excess Reactivity accident analysis, two channels were modeled in PARET; a hot channel representing worst-case conditions inside the core and an average channel representing the rest of the core experiencing "average" conditions. As indicated earlier, the transient was started from an initial power level of 11.5 MW with core coolant flow rate as well as core coolant inlet temperatures set at their LSSS values of 3,200 gpm and 155°F, respectively. Also, pressurizer pressure was at 75 psia (LSSS value). Since the Insertion of Excess Reactivity transient was analyzed from a starting power level of 11.5 MW, the rod run-in that would be initiated by the rod run-in system at 11.5 MW was bypassed and only the high power SCRAM set point of 12.5 MW was modeled. Also, a delay of 150 milliseconds was incorporated

into the control blade SCRAM model so that the control blades would only start to insert 0.15 seconds after the power level had exceeded the SCRAM set point of 12.5 MW.

The results of a step reactivity insertion of 600 pcm (+0.006 Δk/k) are shown below in Figure 10. As expected, due to the higher starting core power level, much lower core coolant flow rate and much higher than normal core coolant inlet temperature conditions assumed for this updated analysis, the peak power during the transient momentarily reaches approximately 37.4 MW compared to a value of approximately 33.0 MW reported in prior SAR analysis for the same 600 pcm step reactivity insertion.

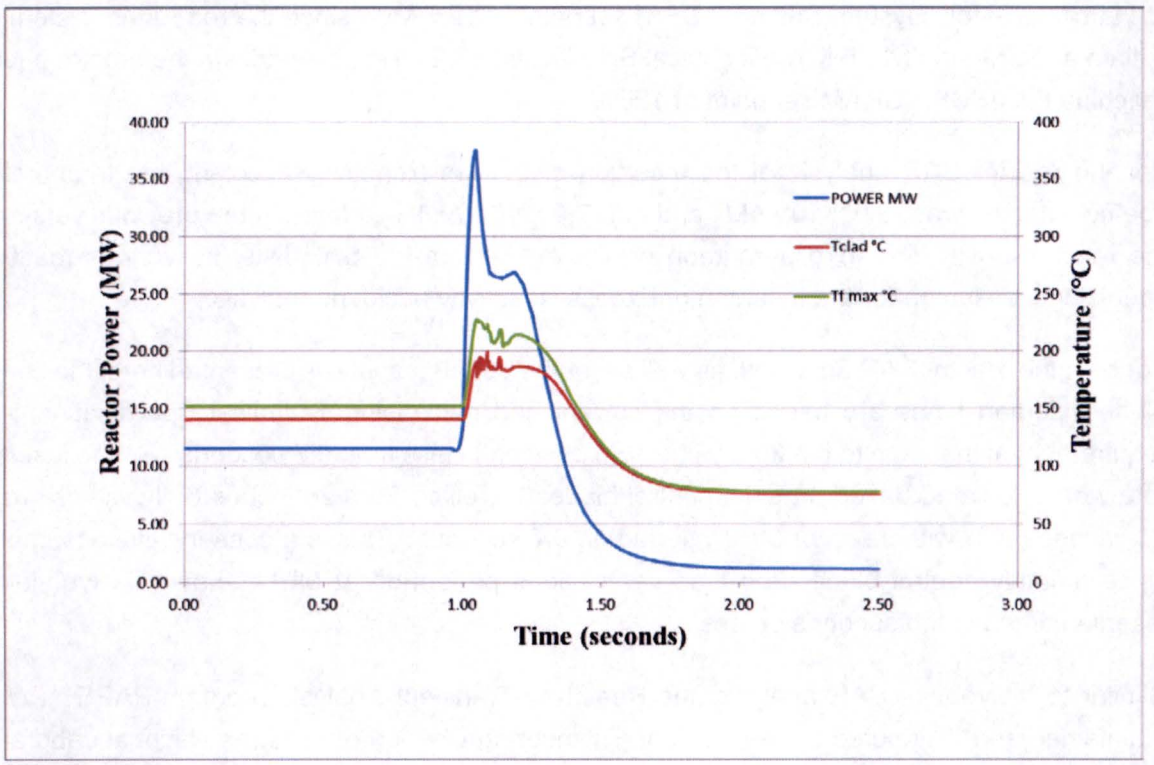

Figure 10. Reactor power, fuel and cladding temperatures vs. time for a positive reactivity step insertion of 600 pcm

The power generation in the target assemblies would follow the same proportional power transient that the reactor core experiences because the target assemblies are driven by the neutron flux generated by the reactor core.

The target rod analysis for the positive reactivity step insertion examines the maximum powered target rod at the beginning and end of a three-week irradiation. A steady state analysis of the three-week irradiation was performed using FRAPCON to establish the initial conditions for the

transient analysis. The FRAPCON analysis assumed that the first and last day of the three week irradiation are at 115% power and the rest of the operating period is at 100% power. The FRAPCON analysis also assumes that the target assembly flow rate is 85% of nominal during the first and last day of operation. Mid-week and weekend shutdowns are also included in the power history for the target assembly. The transient analysis was performed using the FRAPTRAN code. FRAPCON and FRAPTRAN are two NRC-sponsored computer codes that can model the steady state and transient thermal-mechanical behavior of LWR oxide fuel. Phenomena modeled by the codes include heat transfer through fuel and cladding to coolant, cladding elastic/plastic deformation, fuel-cladding mechanical interaction, fission gas release, rod internal pressure, and cladding oxidation.

The FRAPCON steady state analysis defines the burnup, UO_2 and cladding deformation, and fission gas release that form the starting point for the FRAPTRAN analysis. The FRAPTRAN analysis increases the power to 115% and decreases the flow rate to 85% within 40 seconds. Twenty-one seconds later, the 600 pcm (+0.006 Δk/k) step reactivity insertion is simulated. The target cooling water inlet temperature to the target assembly was assumed to be at 102°F (38.9°C) which is higher than the maximum allowable temperature of 90°F (32.2°C) exiting the heat exchanger. The maximum cladding strain occurs with the minimum gap tolerance of [redacted]. The maximum cladding strain also occurs at the end of the three week irradiation due to the effects of burnup on gap closure and fission gas release. The FRAPCON and FRAPTRAN analysis also use the maximum tolerance on the scallop diameter that forms the flow area of the target cartridge. This tolerance results in the minimum velocity consistent with the minimum gap. The analysis also uses the maximum pellet outer diameter, minimum cladding inner diameter, and maximum cladding thickness. The strain transient that the cladding is predicted to undergo during the positive step reactivity insertion is shown in Figure 11. The fractional hoop strain increases from about 0.61% to just over 0.79% but remains under the 1% strain limit.

5a, b, f

[redacted]

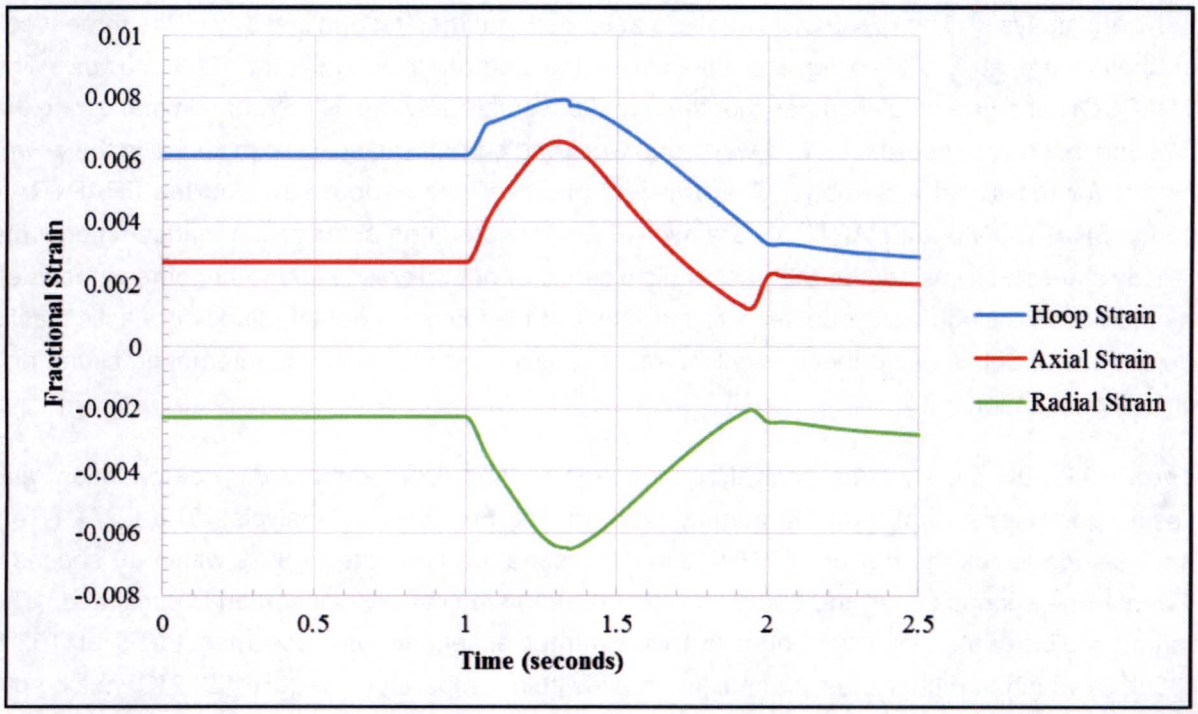

Figure 11. Cladding strains at peak pellet location during 600 pcm reactivity insertion

Maximum target pellet temperatures occur with the maximum gap tolerance of [redacted] rather than the minimum gap tolerance. Burnup effects reduce the gap so that the maximum pellet temperature occurs at the beginning of irradiation. The analysis also uses the minimum pellet outer diameter, maximum cladding inner diameter, maximum cladding thickness, and maximum cladding outer diameter in order to obtain the maximum gap tolerance or to maximize peak pellet temperature. The peak target temperature transient is shown in Figure 12. The peak target temperature increases from 2541°C (4606°F) to 2743°C (4969°F) in less than 0.4 seconds. This peak UO_2 temperature is 97°C (175°F) below the melting temperature of 2840°C (5144°F).

5a, b, f

[redacted]

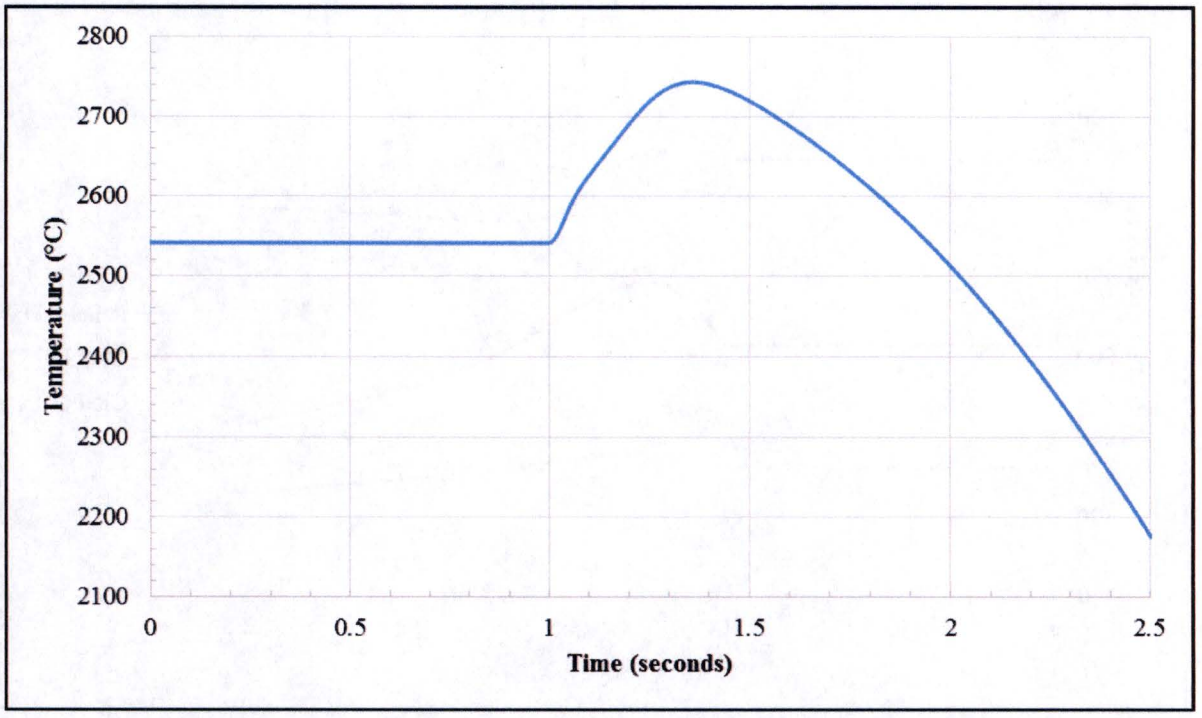

Figure 12. Peak target pellet temperature during 600 pcm reactivity insertion

The pellet outer diameter and cladding inner and outer diameter temperature at the axial location where the peak pellet centerline temperature occurs is shown in Figure 13. The cladding outer diameter temperature shows a modest increase in temperature of around 17°C (31°F). The pellet outer diameter and cladding inner diameter temperatures become more closely coupled due to closure of the gap between the pellet and cladding and an increase in interface pressure. Cladding hoop strain for the [redacted] gap at the end of irradiation goes through a similar transient as for the [redacted] gap but increases from 0.28% to just over 0.60%.

5a, b, f

Peak heat generation within the target pellets is a factor of 3.74 greater than nominal. Heat capacity and thermal resistances result in the surface heat flux at the peak location being only a factor of 1.52 to 1.75 greater than nominal, depending on the initial gap size and burnup conditions. FRAPTRAN assesses critical heat flux (CHF) using one of five different CHF correlations. The MacBeth CHF correlation was chosen because of its validity at low pressures. The MacBeth CHF ratio reaches a minimum value of between 2.25 to 2.53 depending on initial gap size and burnup conditions. The Bernath CHF ratio reaches a minimum of 1.56 to 1.76 depending on the case. No target damage or radiological release would occur from this accident.

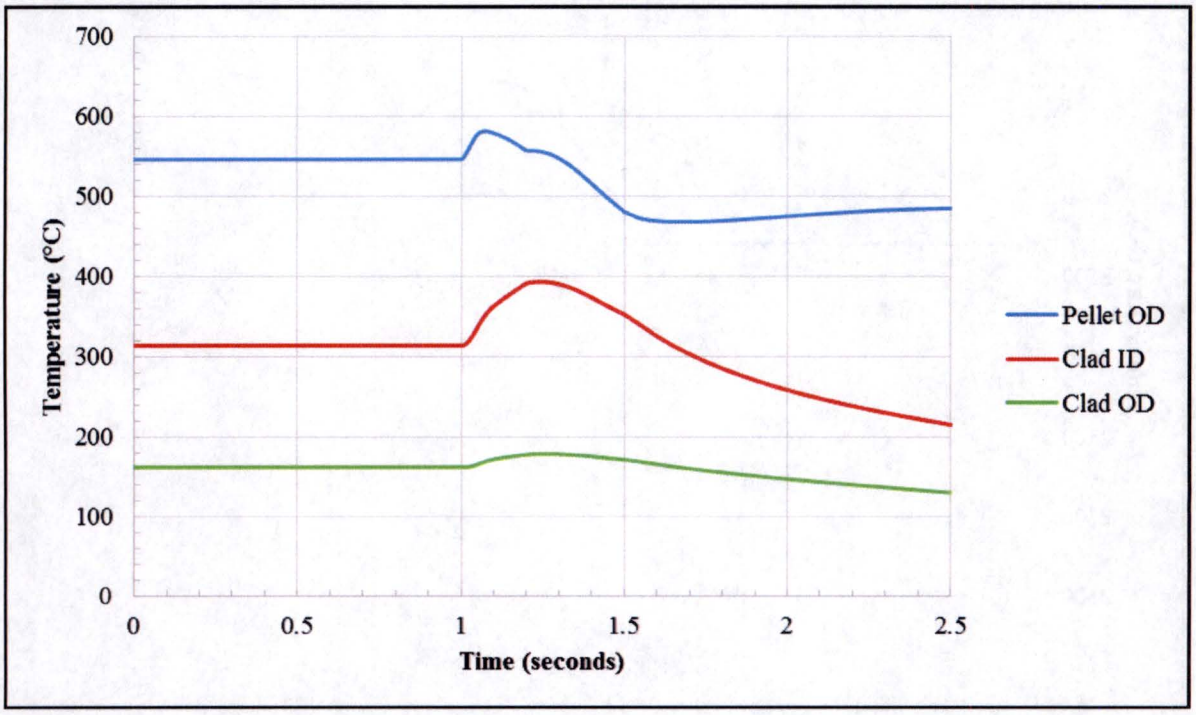

Figure 13. Pellet OD and cladding temperatures at peak pellet location during 600 pcm reactivity insertion

6.2 Control Blade Withdrawal

As presented in section 13.2.2.1.2 of the MURR SAR, a positive reactivity ramp insertion rate of 30 pcm/s, which is the Technical Specification limit on the maximum rate of reactivity insertion for all four shim control blades operating simultaneously, was introduced to the reactor starting at subcritical cold conditions and at an initial power level of 10 MW. For subcritical cold conditions, the short period reactor SCRAM terminates the transient within 150 sec before the power has reached 64 watts. No target pellet or cladding damage would occur at such a low power.

For full power conditions, the high power SCRAM terminates the transient after 4.53 seconds when reactor power rises from 10.0 MW to the 12.5 MW high power SCRAM. The thermal-mechanical performance of the target rod during this transient was analyzed using FRAPCON and FRAPTRAN. The power transient that drives the heat generation in the target rods is shown in Figure 14. The figure includes 1 sec of steady-state operation at 100% power and the power transient after reactor SCRAM.

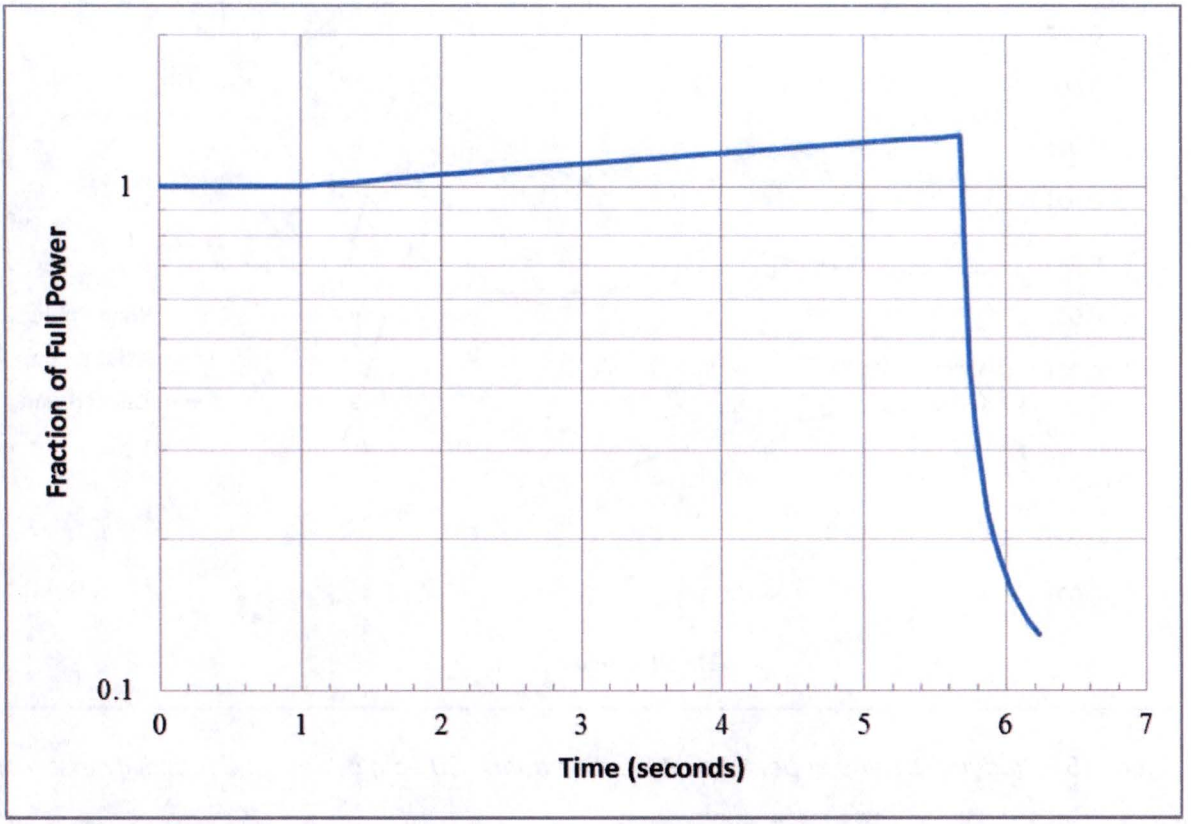

Figure 14. Power transient during 30 pcm per second reactivity insertion

The target rod analysis for the control blade withdrawal examines the maximum powered target rod at the beginning and end of a three-week irradiation. A steady state analysis of the three-week irradiation was performed at 100% power using FRAPCON to establish the initial conditions for the transient analysis. The FRAPCON analysis also assumes that the target assembly flow rate is 100% of nominal during the three-week irradiation. Mid-week and weekend shutdowns are also included in the power history for the target assembly.

The FRAPCON steady state analysis defines the burnup, UO_2 and cladding deformation, and fission gas release that form the starting point for the FRAPTRAN analysis. The maximum cladding strain occurs with the minimum gap tolerance of [redacted] The maximum cladding strain also occurs at the end of the three week irradiation due to the effects of burnup on gap closure and fission gas release. The strain transient that the cladding is predicted to undergo during the control blade withdrawal is shown in Figure 15. The fractional hoop strain increases from about 0.28% to just under 0.61% but remains well under the 1% strain limit.

5a, b, f

[redacted]

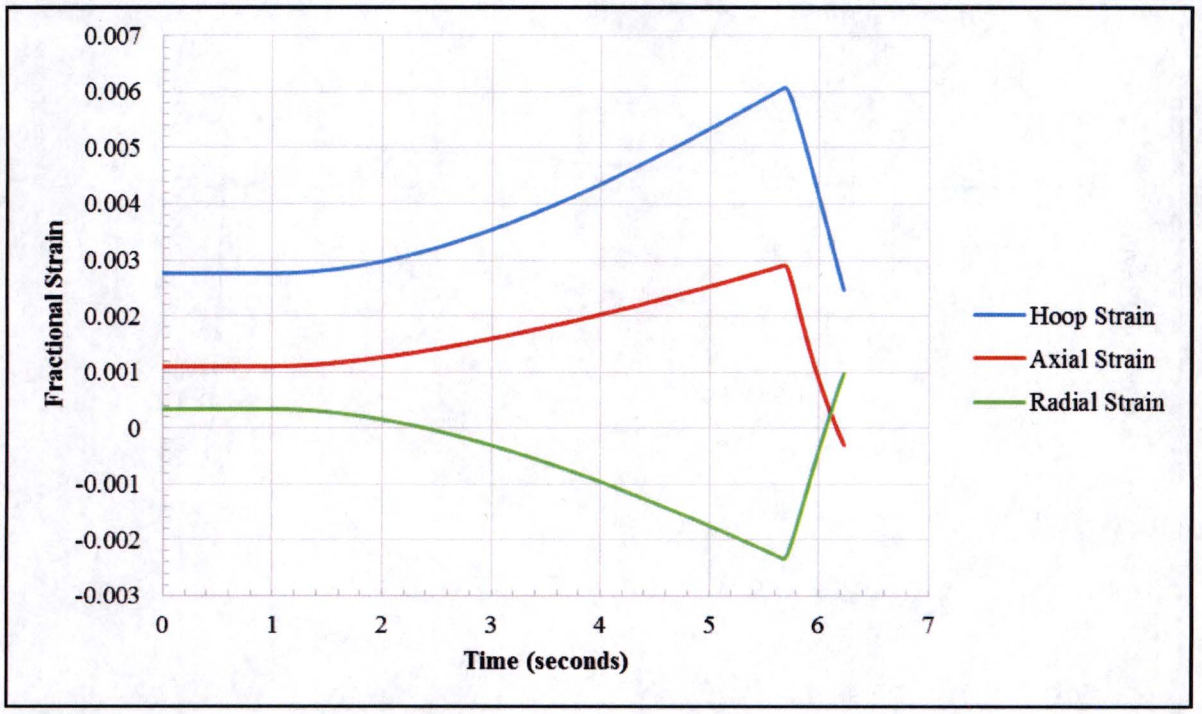

Figure 15. Cladding strains at peak pellet location during 30 pcm per second reactivity insertion

For the case using the [redacted] gap between the pellet and cladding, the pellet centerline temperature increases less than 300°C (540°F) to 2375°C (4307°F) at the end of irradiation. The temperature of the cladding inner diameter increases 27°C (49°F) to just under 315°C (599°F), and the cladding outer diameter temperature increases by less than 8°C (14°F). 5a, b, f

The FRAPTRAN analysis of the [redacted] gap case predicts the maximum pellet temperatures due to the higher thermal resistance between the pellet and cladding. The maximum pellet temperature increases from 2327°C (4221°F) to just over 2563°C (4645°F) at the beginning of irradiation as shown in Figure *16*. The pellet outer diameter and cladding inner and outer diameter temperature at the axial location where the peak pellet centerline temperature occurs is shown in Figure 17. The pellet outer diameter and cladding inner diameter temperatures become more closely coupled due to closure of the gap between the pellet and cladding and an increase in interface pressure. The cladding inner diameter temperature shows a modest increase in temperature of around 35°C (63°F) to just over 321°C (610°F). Cladding fractional hoop strain goes through a similar transient as shown in Figure 15 but increases from 0.13% to 0.14%. No target damage or radiological release would occur from this accident. 5a, b, f

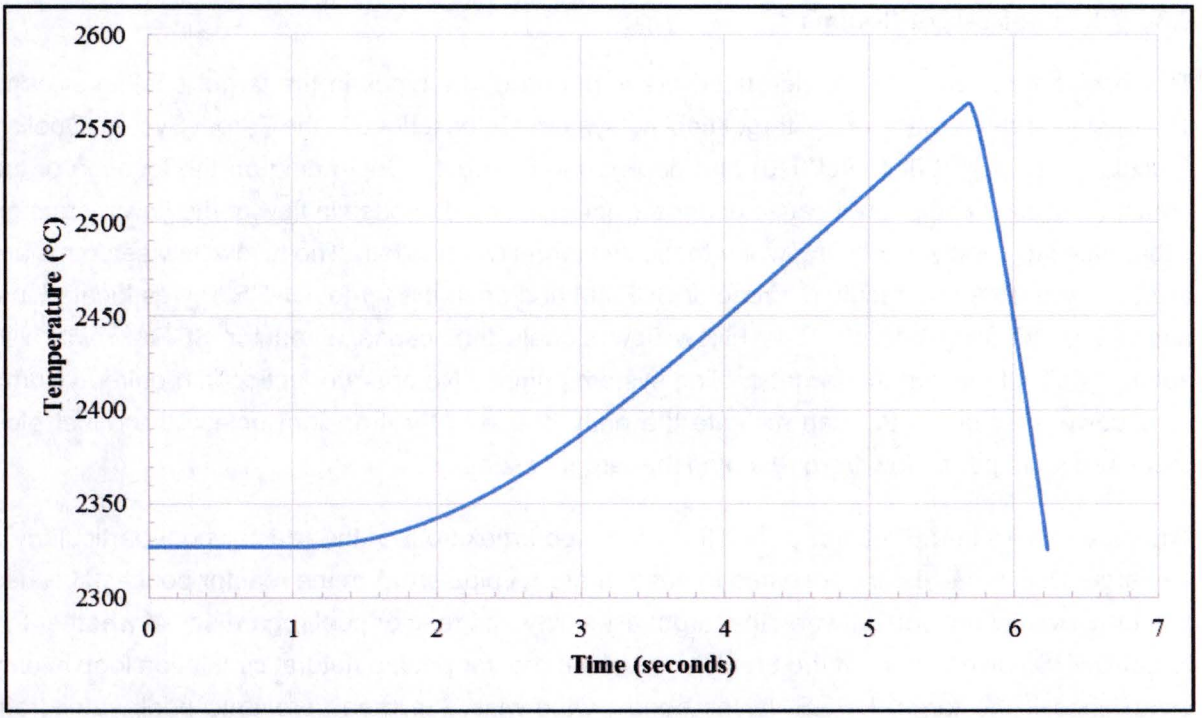

Figure 16. Peak target pellet temperature during 30 pcm per second reactivity insertion

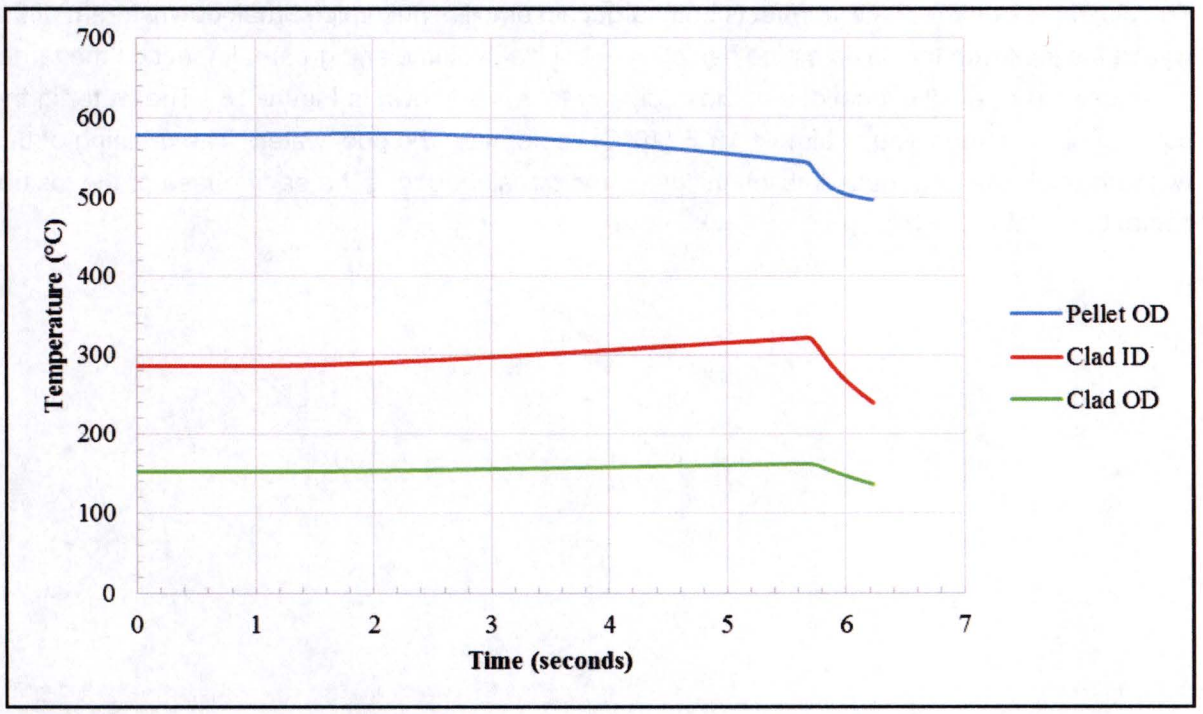

Figure 17. Pellet OD and cladding temperatures at peak pellet location during 30 pcm per second reactivity insertion

6.3 Loss of Target Coolant

This accident assumes a double-ended break of one of the pipes in the target cooling system. The design and operation of the target cooling system are described in the Target System Cooling Calculation Report (30441R00019) and depicted in Figure 1. Depending on the location of the break, the loss of coolant will cause either an increase or a decrease in flow at the flow meters on either pipe leg supplying cooling water to the two target assemblies. The hi/low flow setpoints are at 115% and 85% and result in a reactor SCRAM and open the target DHRS valves located just above the refueling bridge. The hi/low flow signals that cause a reactor SCRAM will also automatically shutdown the target cooling system pumps. No operator action is required. Pump coastdown after pump trip can mitigate the early phase of the transient unless the offset pipe break prevents pump flow from reaching the target assembly.

The pipe breaks in the reactor pool differ from pipe breaks out of the reactor pool particularly if the target DHRS valves are assumed to not operate. A pipe break in the reactor pool establishes a natural circulation loop between the target assembly and reactor pool regardless of whether the target DHRS valves open. If the break is out of the reactor pool, a natural circulation loop is only established if the target DHRS valves open. Otherwise, the break prevents pool water from reaching the target assembly inlet and establishing a natural circulation loop.

The pipe break before the wye affects both target assemblies but a pipe break downstream of the wye at the joint with the flexible pipe has a lower cold leg volume and greater impact on the target assembly. The relative locations of these pipe breaks are shown in Figure 18. The water in the cold leg of the supply line is almost 18°F (10°C) cooler than the pool water. The draining of this water through the target assemblies mitigates the transient during the early phase of the loss of coolant accident (LOCA).

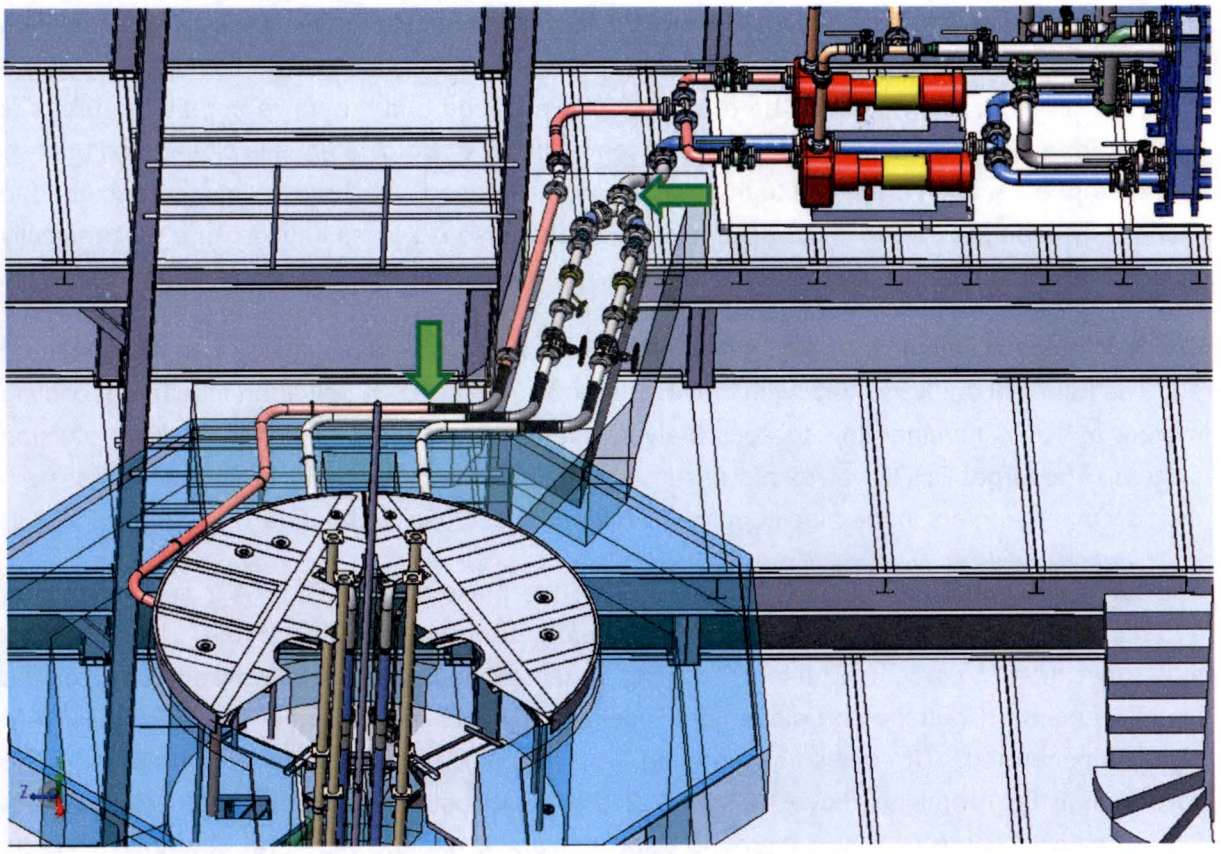

Figure 18. Pipe break locations out of the reactor pool

Pipe breaks out of the reactor pool are covered in Section 6.3.1 and pipe breaks in the reactor pool are covered in Section 6.3.2.

6.3.1 Pipe Break out of the Reactor Pool

The pipe break out of the reactor pool just after the flexible pipe is a more credible pipe break than other locations closer to the target assembly because the joint is more vulnerable and the remaining pipe is of welded construction. The upper bridge structure protects the pipes where they bend downward into the reactor pool. The break is analyzed to occur in the supply line to target assembly (TA) 2 because it has the target rod with the highest power density, and the target rod with the highest power in addition to being the target assembly with the most power.

The LOCA for the Selective Gas Extraction (SGE) target was modeled using RELAP5 mod3.3 patch 03. RELAP5 was developed by the NRC to analyze thermal-hydraulic transients in pressurized water reactors. It can be used to analyze a variety of geometries and was used to analyze the LOCA and Loss of Flow Accident (LOFA) in Sections 13.2.3 and 13.2.4 of the MURR SAR for relicensing. The RELAP5 model for this accident includes both target assemblies, target cooling system pump and heat exchanger, and target DHRS valves. The double-ended guillotine

rupture is modeled with three valves – two of the valves connect to the reactor pool on either side of the break, and the third valve connects the two ends of the pipe across the break. Prior to accident initiation, the valves to the reactor pool are closed and the valve across the break is open. When the break is initiated, the valve connecting the two pipe ends is closed and the two valves from each end connected to the reactor pool is opened. All three valves are assumed to completely change position in 0.5 seconds which is a reasonable assumption for a mechanically induced failure that displaces the two ends of the pipe since the piping is not at high pressure.

The flow transient caused by a LOCA resulting from a double ended pipe break is shown in Figure 19. The transient analysis starts with the reactor and target at 100% power and the target cooling system at 100% nominal flow to accurately simulate the expected response of the protection system. The target DHRS valves are assumed to not operate. The break causes an increase in the flow measurement in the pipe supplying TA 2 and a decrease in the flow rate supplying TA 1.

The reactor is scrammed at 0.05 seconds when the mass flow rate to TA 2 is greater than 115 percent. A low flow signal occurs shortly thereafter at 0.08 seconds for TA 1 when its flow rate is less than 85 percent. The target cooling system pumps are automatically shutdown on the high flow alarm. Control blade movement is delayed by 0.15 seconds after the reactor SCRAM signal is generated. The mass flow entering TA 2 falls quickly because of the pipe break. The flow through TA 1 remains above 1.0 kg/s (2.2 lb/s) for almost 20 seconds. The flow through TA 2 drops below 1.0 kg/s (2.2 lb/s) at around 9 seconds and experiences several slow flow reversals between 10 and 40 seconds after which boiling and chugging within both target assemblies is predicted.

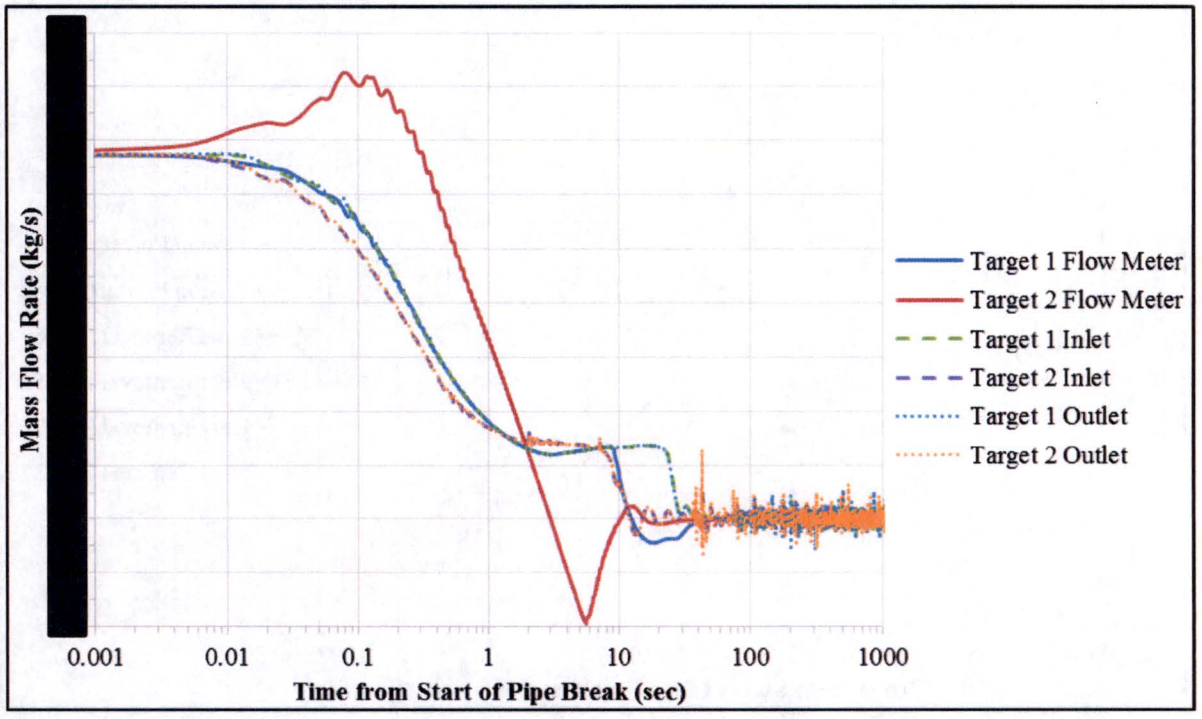

5a, d, e, f

Figure 19. Mass flow transient during LOCA out of the reactor pool without target DHRS valves

In TA 2, rod 17 has the maximum peak power density and rod 22 has the maximum rod power. In TA 1, rod 5 has the maximum peak power density and rod 6 has the maximum rod power though both rods are lower in power than the rods in TA 2. The heat generation in the target rods is shown in Figure 20. The heat generation drops at around 0.20 seconds when the control blades start inserting. The heat removal from the target rods presented in Figure 20 shows that stored energy removal is significant over the first 10 seconds. Mass flow oscillations due to chugging and boiling are also reflected in the oscillations in heat removal.

Coolant temperatures at the inlet and outlet of the two target assemblies are presented in Figure 21. Mass flow out of the target assemblies due to boiling are represented by outlet temperatures between 70 and 100°C (160 and 212°F). Mass flow back into the target assemblies are represented by the lower bounds of the temperature oscillations around 50°C (120°F). These flow oscillations also move water and thermal energy to the target assembly entrance which slowly raises that temperature.

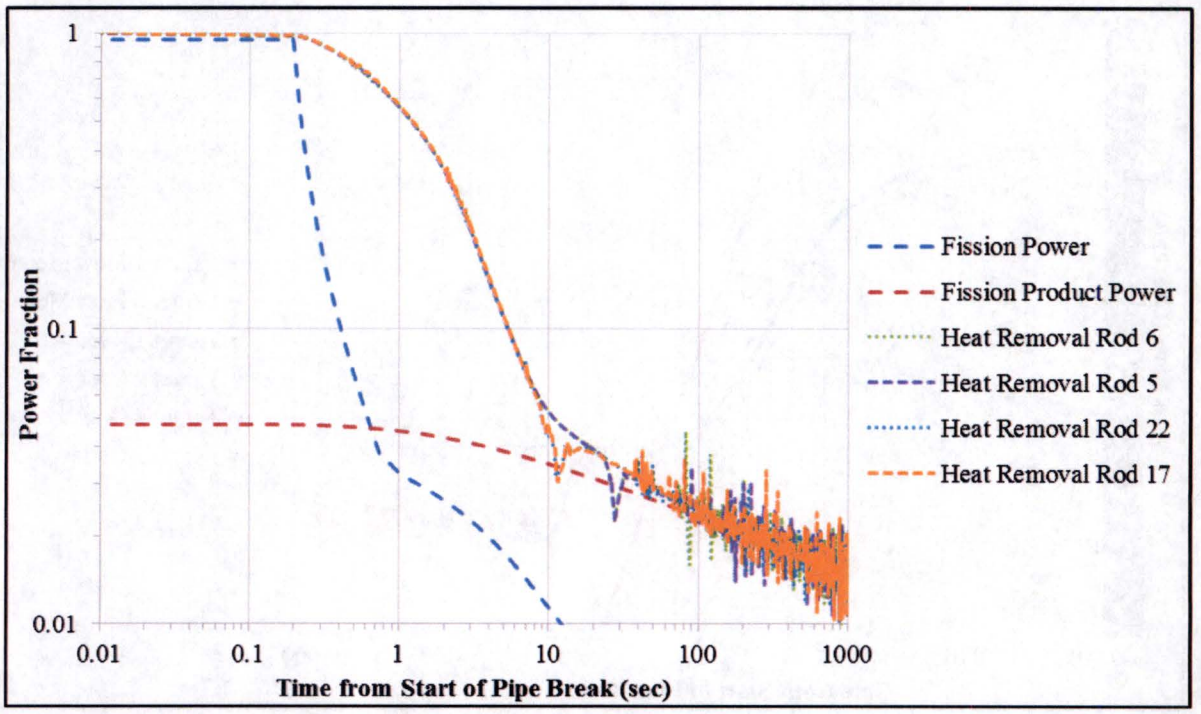

Figure 20. Target power during a LOCA out of the reactor pool without target DHRS valves

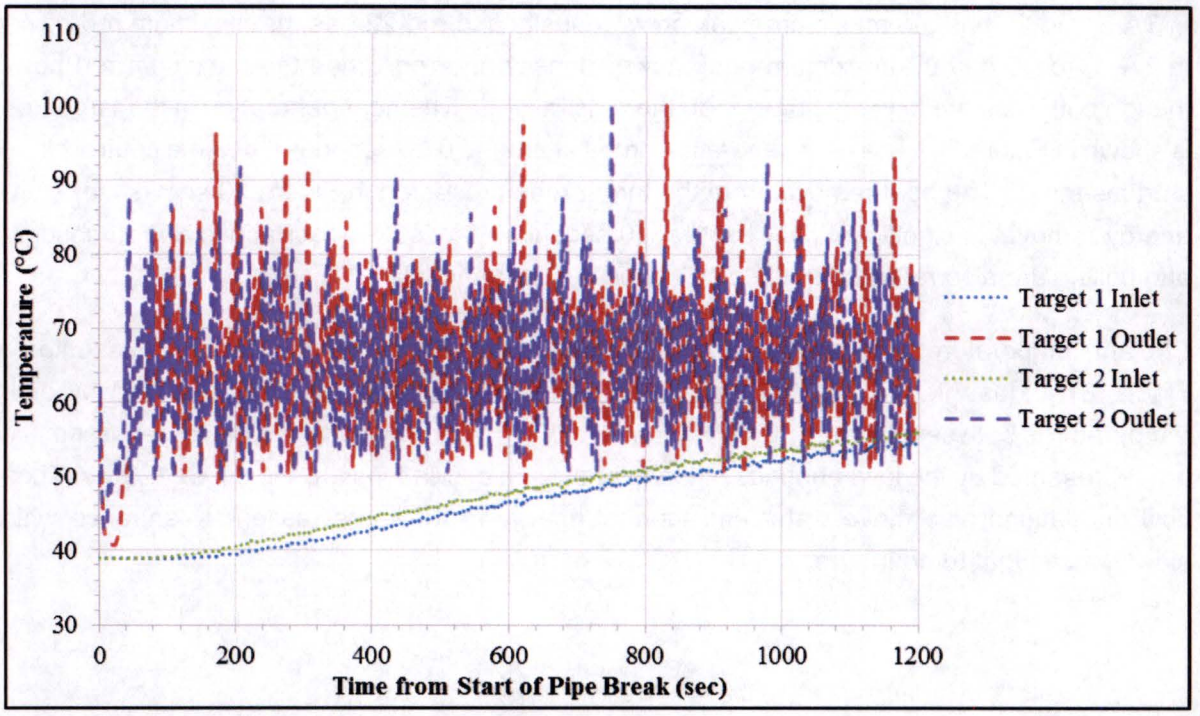

Figure 21. Coolant temperatures during a LOCA out of the reactor pool without target DHRS valves

Pellet centerline temperatures do not increase during this LOCA because of the reactor SCRAM signal at 0.05 seconds, the UO_2 heat capacity, and the water flow through the target caused by draining of the cooling line. The maximum temperatures of the cladding inner diameter (ID) are shown in Figure 22. The cladding inner diameter temperature increases by 3.0°C (5.4°F) prior to control blade insertion and afterwards, is lower than normal temperature. The increases in cladding inner diameter temperature at around 10 and 30 seconds coincide with the decreases in flow rate at those times. Boiling within the target assemblies keeps the maximum cladding temperature just above saturation temperature.

Because the pellet and cladding temperatures are near normal values, all cladding stresses and strains are also normal. Therefore, there is no cladding breach and no release of radioactivity associated with this LOCA.

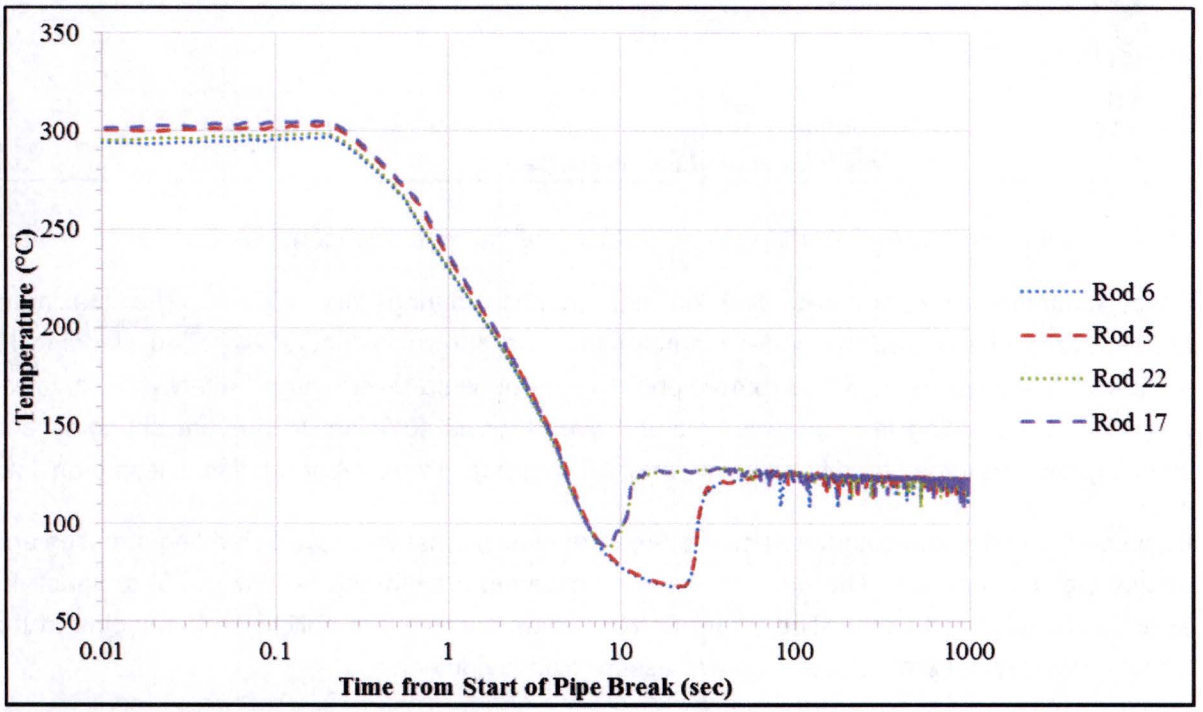

Figure 22. Maximum cladding ID temperatures during a LOCA out of the reactor pool without target DHRS valves

If the one of the two target DHRS valves for each target assembly were to operate, the consequences of the LOCA out of the reactor pool are greatly improved. The flow transient due to a LOCA out of the reactor pool with the target DHRS valves working is shown in Figure 23. The target inlet flow is the same as the target outlet flow and a small natural circulation flow is established after 20 seconds. TA 1 flow rate is higher around 10 seconds due to a small contribution of pump coastdown through the intact supply line to TA 1.

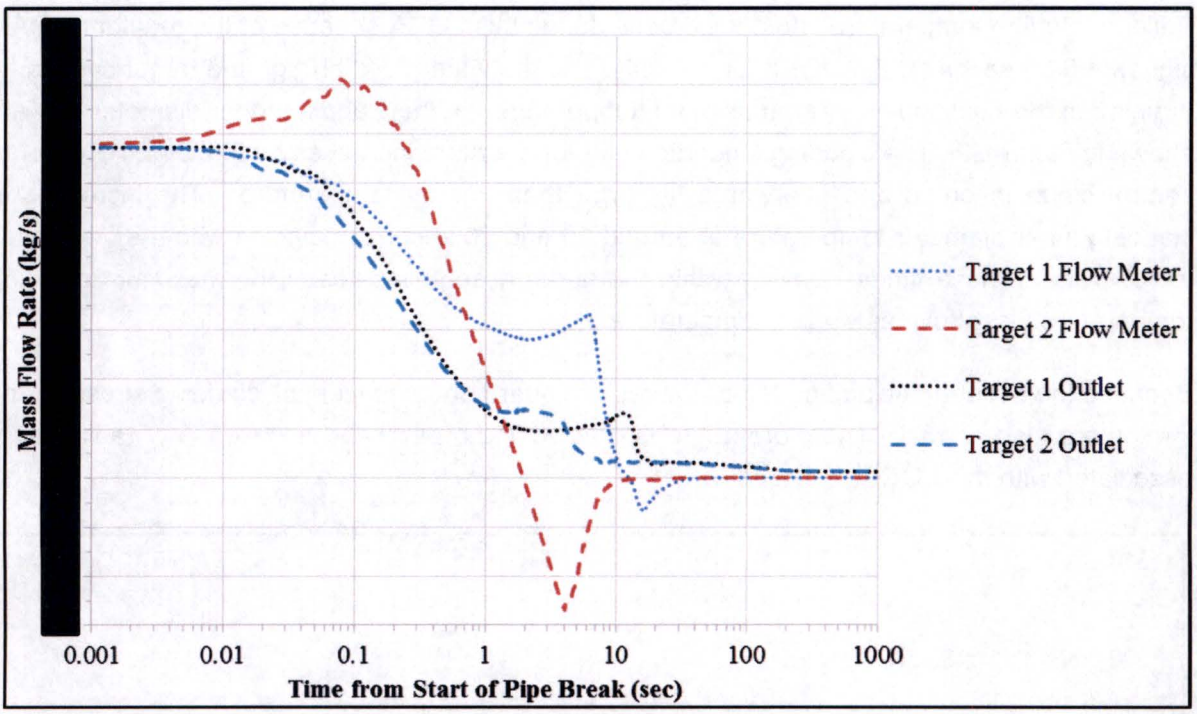

5a, d, e, f

Figure 23. Mass flow transient during a LOCA out of the reactor pool with target DHRS valves

Pellet centerline temperatures also do not increase during this LOCA. The maximum temperatures of the cladding inner diameter (ID) are shown in Figure 24. The cladding ID temperature increases by 3.0°C (5.4°F) prior to control blade insertion and afterwards, is lower than normal operating temperature. Natural circulation is sufficient to prevent chugging and cladding temperatures steadily decrease after 20 seconds. Peak vapor fraction is less than 1%.

Because the pellet and cladding temperatures are near normal values, all cladding stresses and strains are also normal. Therefore, there is no cladding breach and no release of radioactivity associated with this LOCA. The target DHRS valves can prevent boiling and chugging in the target assembly but are not necessary to assure cladding integrity.

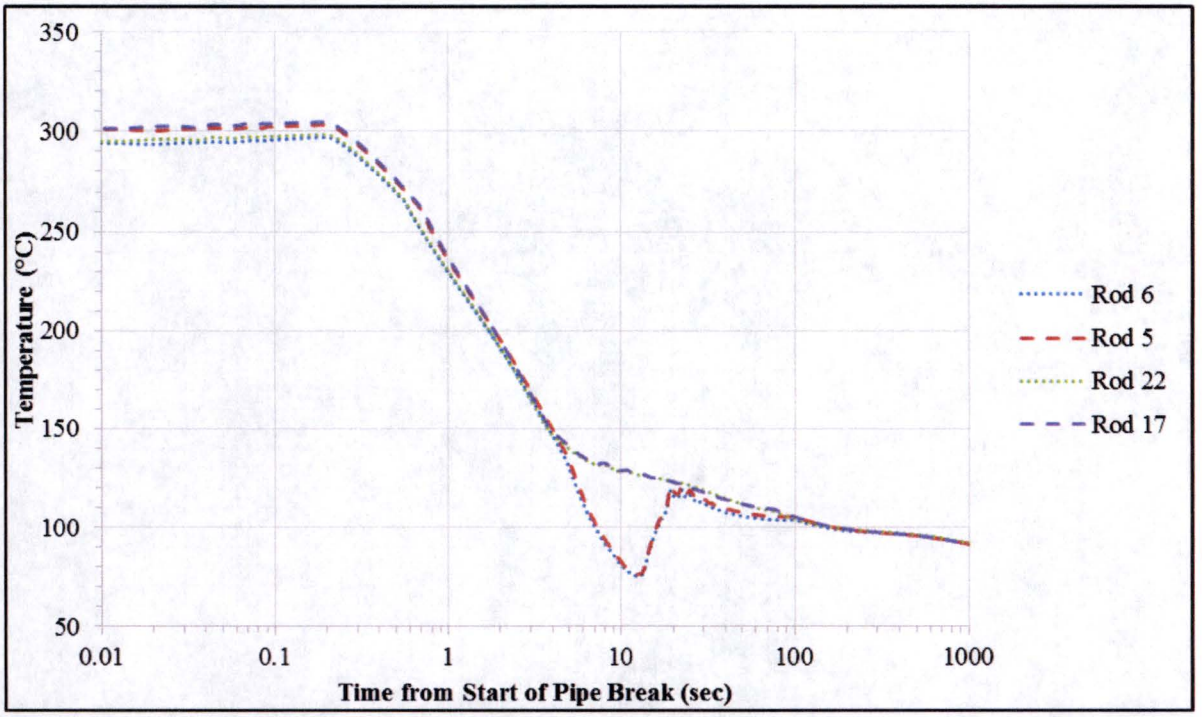

Figure 24. Maximum cladding ID temperatures during a LOCA out of the reactor pool with target DHRS valves

6.3.2 Pipe Break in the Reactor Pool

The target cooling lines supplying water to the target assemblies are protected by the upper bridge structure above the pool and the refueling bridge located below the normal pool water level. The cooling lines also have lateral supports and are joined to the target assembly by a flexible joint. It is nearly incredible to postulate a mechanistic failure of these cooling pipes which results in a complete offset rupture within the assumed rupture time of 0.5 sec. If the break occurs up near the target DHRS valves then it is essentially the same as opening the target DHRS valves. The worst possible break location is the connection between the inlet pipe welded to the target housing and the flexible pipe as shown in Figure 25. Direct mechanical interaction in this area is very unlikely due to the congestion around this elevation.

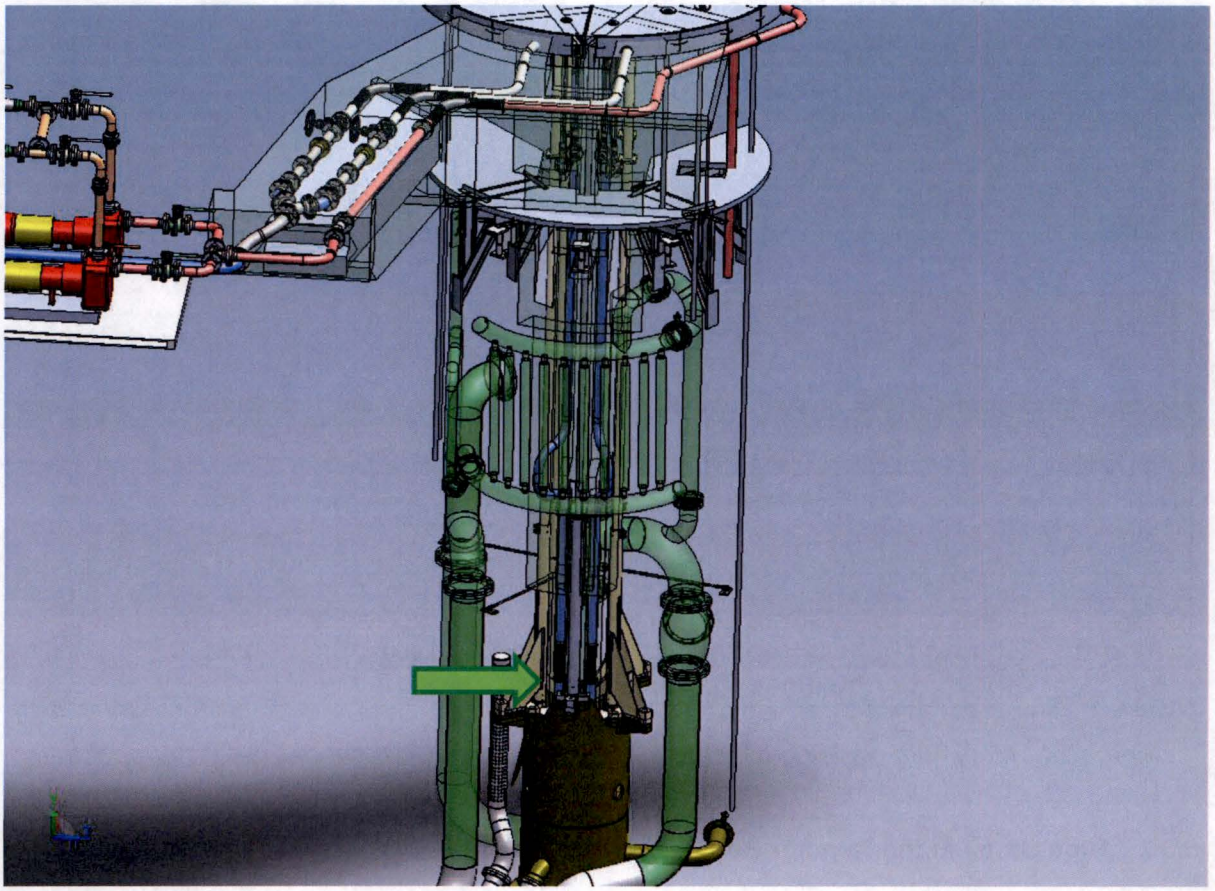

Figure 25. Pipe break location in reactor pool

The LOCA in the reactor pool used the same RELAP5 model as the LOCAs out of the reactor pool except that the break location was relocated as shown in Figure 25. The break time to completely offset the rupture was also kept at 0.5 seconds although it is more likely that the break time would be either longer underwater or less than a complete offset rupture.

The flow transient caused by a LOCA in the reactor pool resulting from a double ended pipe break is shown in Figure 26. The transient analysis starts with the reactor and target at 100% power and the target cooling system at 100% nominal flow to accurately simulate the expected response of the protection system. The target DHRS valves are assumed to not operate though their operation would be ineffective in this accident. The break causes an increase in the flow measurement in the pipe supplying TA 2 and a decrease in the flow rate supplying TA 1.

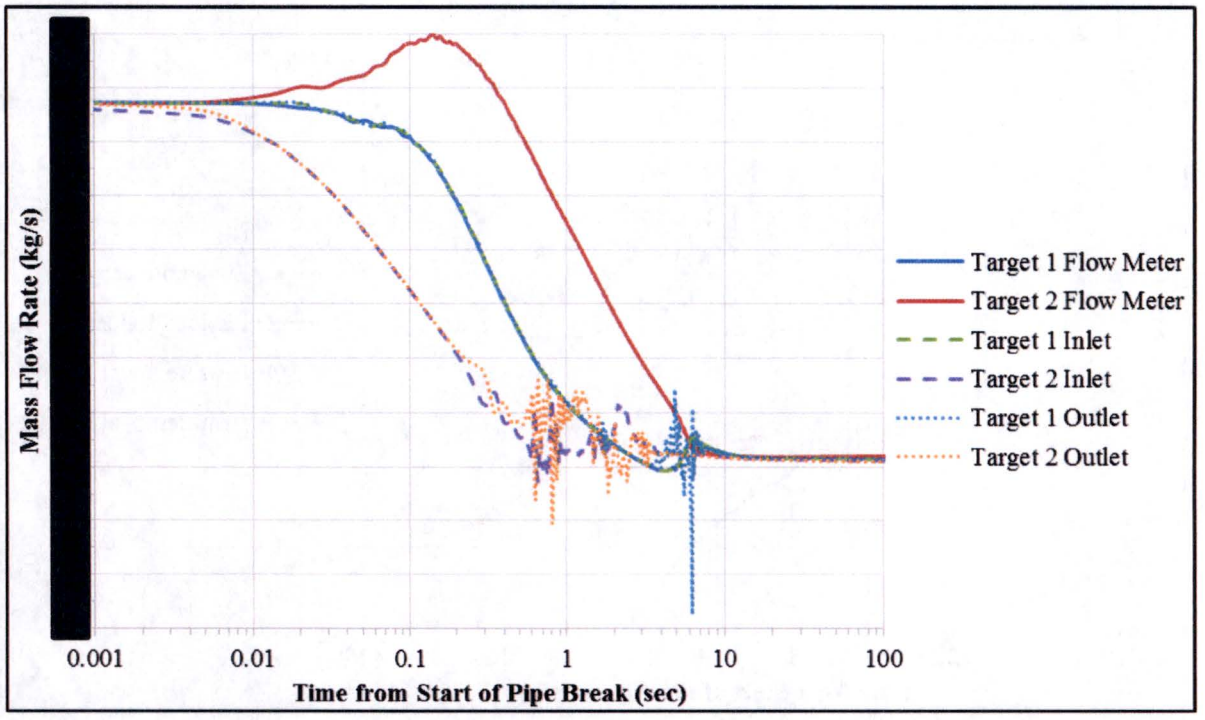

5a, d, e, f

Figure 26. Mass flow transient during a LOCA in the reactor pool

The reactor is scrammed at 0.09 seconds when the mass flow rate to TA 2 is greater than 115 percent. A low flow signal occurs shortly thereafter at 0.13 seconds for TA 1 when its flow rate is less than 85 percent. The target cooling system pumps are automatically shutdown on the high flow alarm. Control blade movement is delayed by 0.15 seconds after the reactor SCRAM signal is generated. The mass flow entering TA 2 falls quickly because of the pipe break. The flow through TA 2 drops to zero at around 0.6 seconds and experiences several boiling and chugging oscillation for the next few seconds. The flow through TA 1 remains above zero for about 3 seconds before it also experiences some boiling and chugging oscillations. Natural circulation through TA 2 after 6 seconds is sufficient to prevent further boiling and chugging.

The heat generation in the target rods is shown in Figure 27. The heat generation drops at around 0.24 seconds when the control blades start inserting. Brief periods of transition and film boiling occur at the high heat flux locations of the target rods. The heat removal from the target rods presented in Figure 27 shows that stored energy removal is significant over the first 10 seconds. Mass flow oscillations due to chugging and boiling are also reflected in the oscillations in heat removal and occur while significant stored energy remains to be removed.

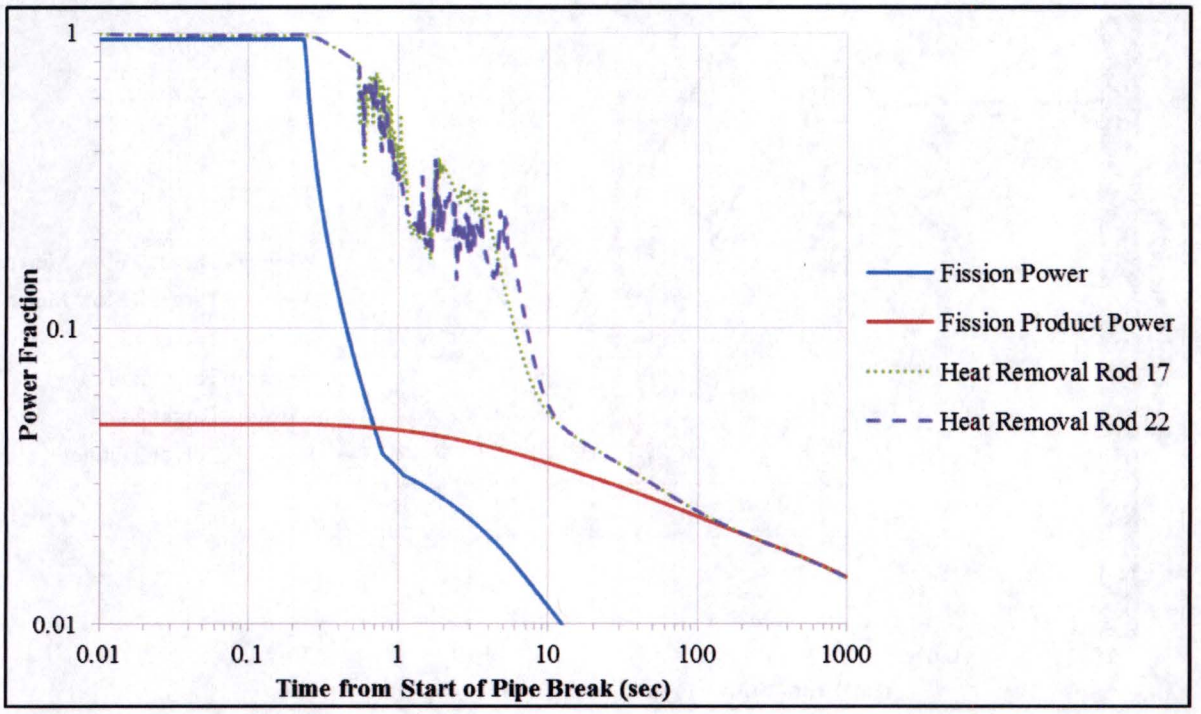

Figure 27. Target power during a LOCA in the reactor pool

The maximum temperatures of the cladding inner diameter (ID) and coolant entering and exiting TA 2 are shown in Figure 28. Cladding temperatures start experiencing rapid increases at around 0.6 seconds which corresponds to the rapid drop in flow rate. Peak cladding temperatures reach 849°C (1560°F) in target rod 22 and 827°C (1520°F) in target rod 17. Peak cladding temperatures in rods 5 and 6 steadily decline after reactor scram except for a brief temperature excursion of around 100°C (180°F) between 6 and 7 seconds.

A FRAPTRAN analysis of cladding integrity during this LOCA in the reactor pool transient was performed using minimum and maximum pellet-clad gap tolerances of 36 microns (1.42 mils) and 64 microns (2.52 mils). Cladding outer diameter (OD) temperatures as a function of time and axial location were obtained from RELAP5 and used as the boundary condition for the FRAPTRAN analysis. FRAPCON results used in the reactivity transients in Section 6.2 were used to define the burnup and fission gas release inputs for FRAPTRAN at beginning of life (BOL) and end of life (EOL) conditions. The maximum hoop strain occurs at EOL conditions in target rod 22 with the maximum gap tolerance of 64 microns (2.52 mils). The cladding temperatures used in the FRAPTRAN analysis for rod 22 are presented in Figure 29. The maximum hoop strain of 0.54% at the peak strain location along with the radial and axial strains at that location are presented in Figure 30. These strains are much less than the 1% strain criteria so that cladding integrity is maintained. The external pressure at BOL conditions is less than 15% greater than the internal pressure so that buckling of the cladding is not possible.

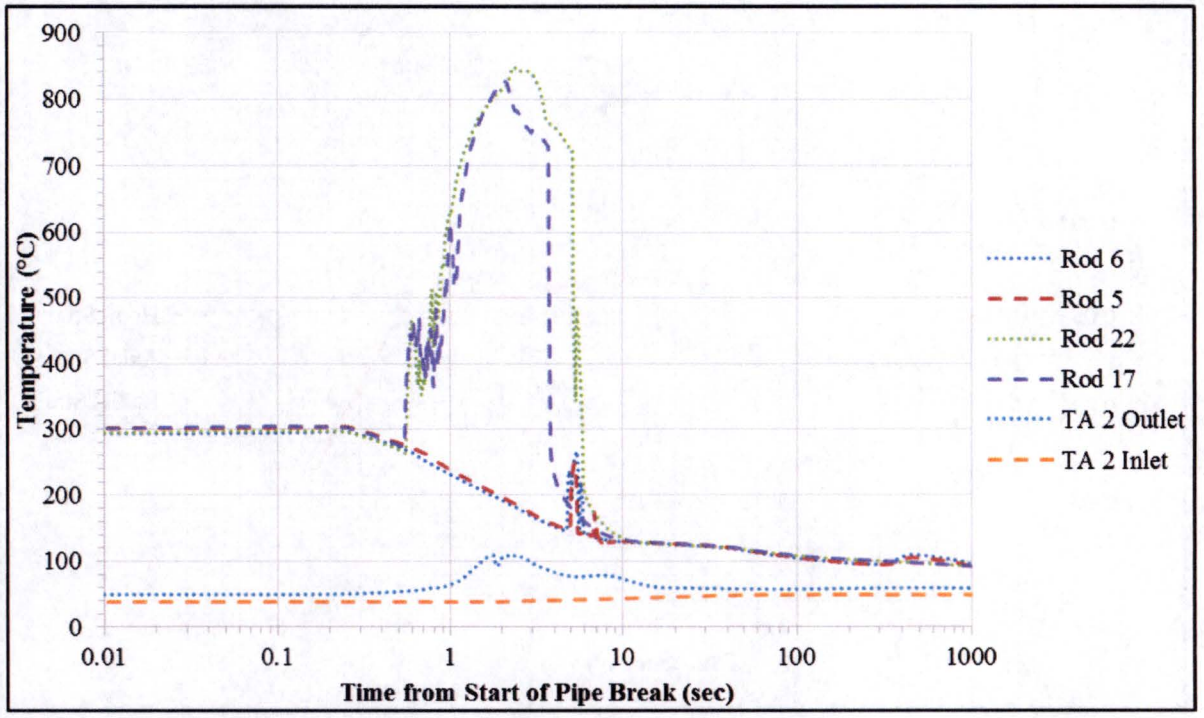

Figure 28. Maximum cladding ID and coolant temperatures during a LOCA in the reactor pool

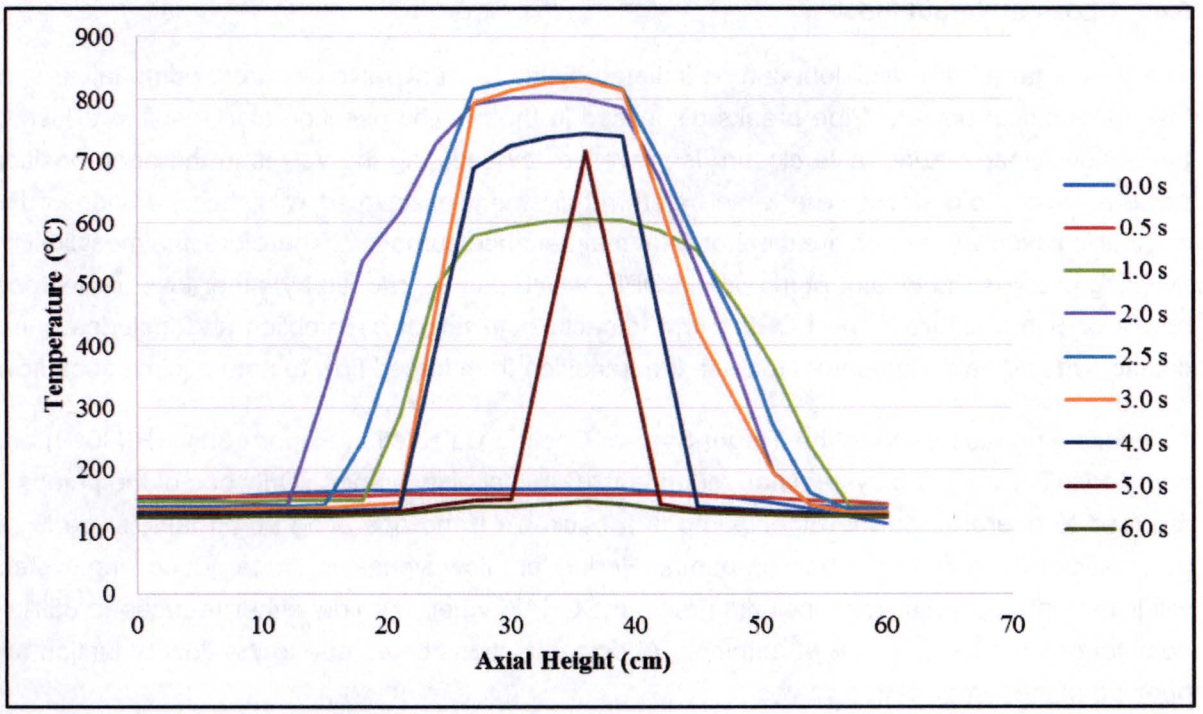

Figure 29. Maximum cladding OD temperature profile in rod 22 during a LOCA in the reactor pool

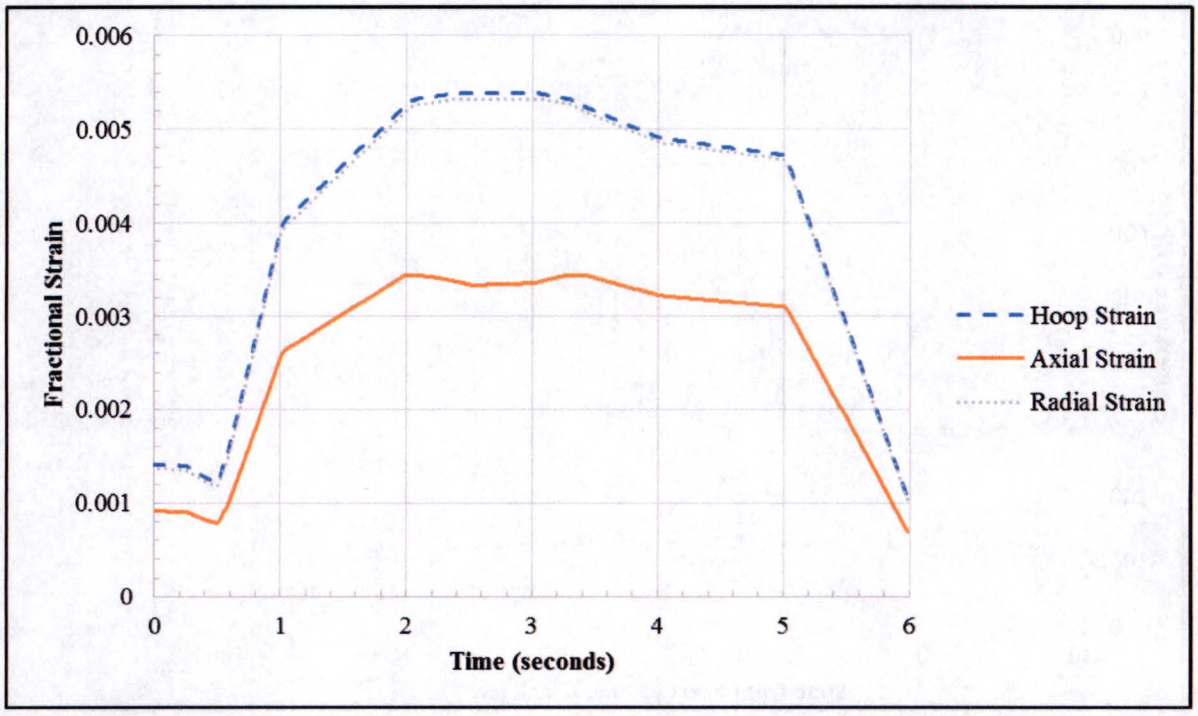

Figure 30. Cladding fractional strains in rod 22 during a LOCA in the reactor pool

6.4 Loss of Target Flow

The loss of target flow accident can be initiated by inadvertent valve closures, pump failures, or loss of electrical power. Pipe breaks discussed in the previous section also result in a loss of target flow. Inadvertent valve closure is prevented by securing the valves in the open position using a locking pin since there is no safety requirement associated with the operation of the manual isolation valves and are there only for maintenance purposes. Therefore, the most limiting initiating event is the loss of pump flow (LOPF) which can be caused by either loss of electrical power or pump failure. The LOPF event impacts both target assemblies and includes pump coastdown and fluid momentum to ease the transition from forced flow to natural circulation flow.

As shown and discussed in the Target System Cooling Calculation Report (30441R00019) and depicted in Figure 1, the system has redundant 100% capacity pumps. Only one of the pumps is required to operate and the other pump is a backup. If the operating pump fails, there is no automatic switchover to the backup pump. Redundant flow signals in the target cooling system will initiate protective actions including reactor SCRAM when the flow either reduces to 85% of nominal or increase to 115% of nominal. Additional actions taken due to the flow reduction are opening of the target DHRS valves.

The LOPF was modeled using RELAP5 mod3.3 patch 03. The RELAP5 model is the same model used for the LOCA analysis described in Section 6.3.

The flow transient caused by this LOPF is shown in Figure 31. The transient analysis starts with the target cooling system at 100% power and 100% nominal flow to accurately simulate the expected response of the protection system. The LOPF accident is assumed to include a loss of secondary flow as one would expect during a loss of site power. The analysis assumes that the target DHRS valves do not open. The LOPF causes a decrease in the flow measurement in the pipes supplying TA 1 and TA 2. Pump coastdown takes about 10 seconds to complete. The reactor is scrammed at 0.14 seconds when the mass flow rate drops below 85%. Control blade movement is delayed by 0.15 seconds after the reactor SCRAM signal is generated. As natural circulation progresses, the colder water in the target cooling system is slowly replaced with water at pool temperature which eventually results in a decline in natural circulation flow at around 600 seconds.

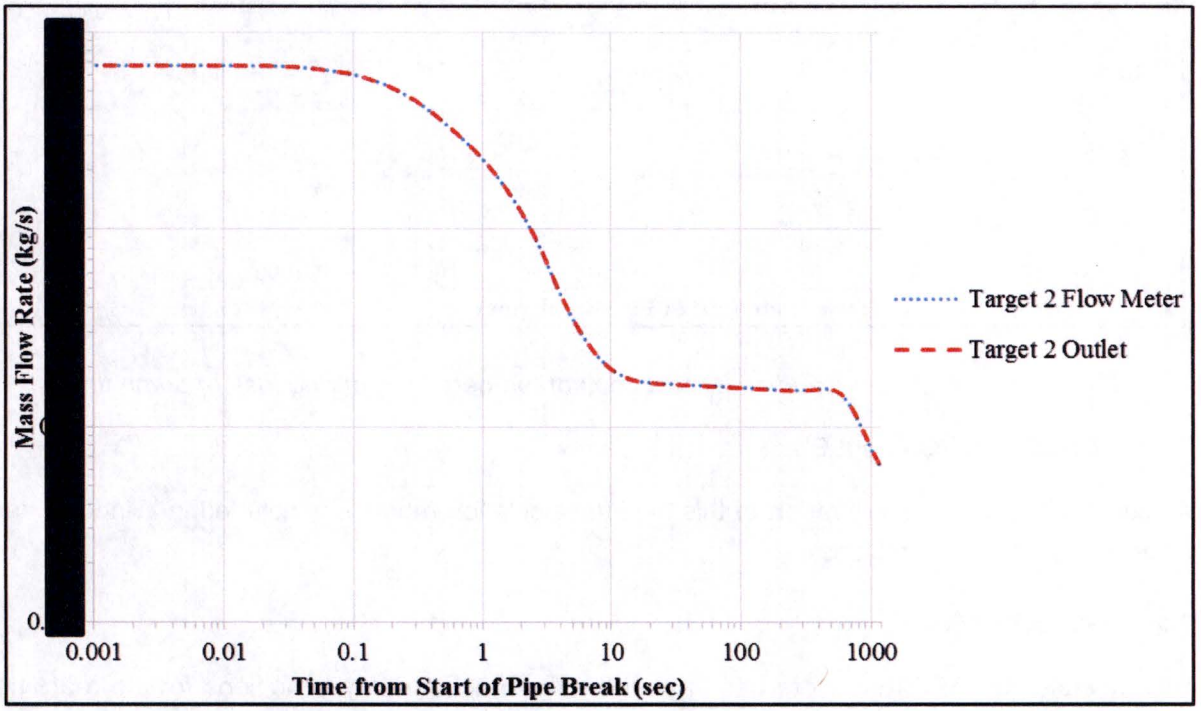

5a, d, e, f

Figure 31. Mass flow transient during loss of pump flow

Maximum cladding ID temperatures and coolant temperatures are shown in Figure 32. Peak cladding temperatures rise slightly by 2.0°C (3.6°F) but then steadily decline after reactor SCRAM. Coolant exit temperature from TA 2 rises slightly at around 5 seconds and again after 600 seconds. At 600 seconds the inlet temperature starts to rise as reactor pool water has mixed with the cooler target cooling water. Eventually the target inlet temperature will reach the maximum pool temperature of 50°C (120°F) at which point further increase in temperatures will cease.

Because the pellet and cladding temperatures are near normal values, all cladding stresses and strains are also normal. Therefore, there is no cladding breach and no release of radioactivity

associated with this LOPF. The target DHRS valves can improve the natural circulation cooling in the target assembly but are not necessary to assure cladding integrity.

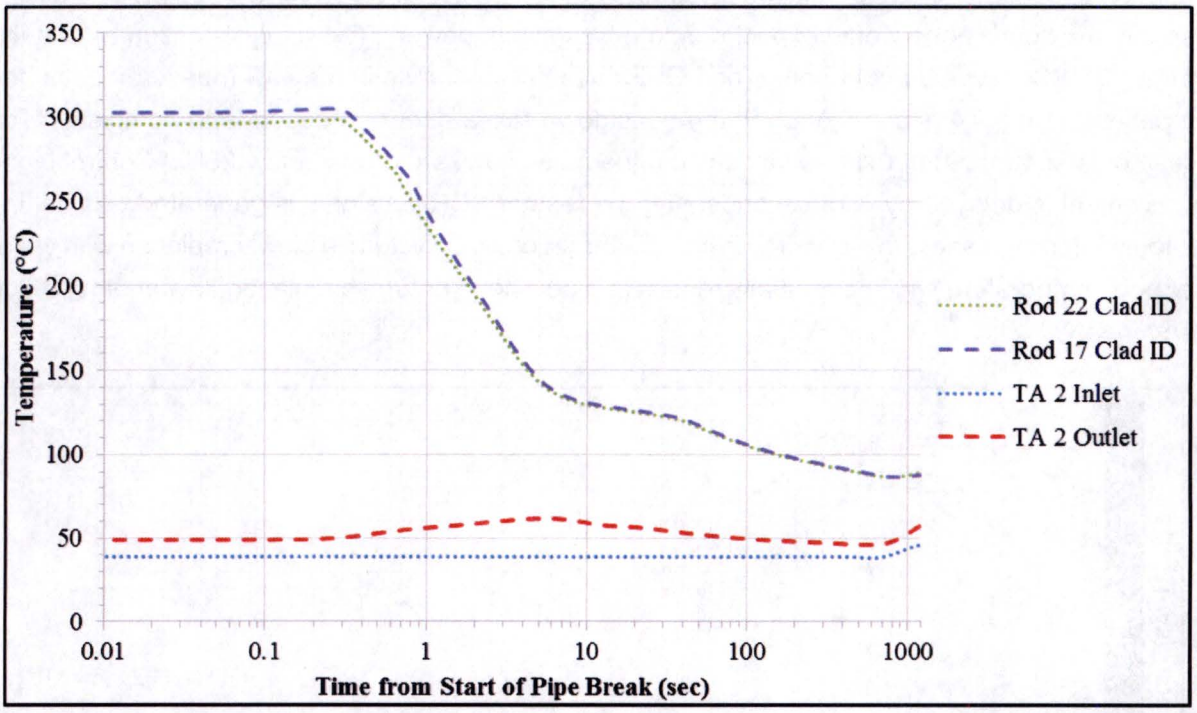

Figure 32. Maximum cladding ID and coolant temperatures during loss of pump flow

7 CALCULATIONS FILES

All computer files used in support of this design calculation report are included in Windchill and listed in the following sections.

7.1 RELAP5 Files

Steady state RELAP5 runs were used to set the thermal boundary conditions for the reactivity transients in FRAPCON. The following filenames were used with file extensions of <filename>.inp for input and <filename>.out for output.

- 1thruC_10.0MW_36SSnomF - constant 10 MW (100%) power with [redacted] gap and nominal flow
- 1thruC_10.0MW_50SSnomF - constant 10 MW (100%) power with 50 μm gap and nominal flow
- 1thruC_10.0MW_64SSnomF - constant 10 MW (100%) power with [redacted] gap and nominal flow

5a, b, f

[redacted]

- 1thruC_11.5MW_36SSnomF - constant 11.5 MW (115%) power with [redacted] gap and nominal flow
- 1thruC_11.5MW_50SSnomF - constant 11.5 MW (115%) power with 50 μm gap and nominal flow
- 1thruC_11.5MW_64SSnomF - constant 11.5 MW (115%) power with [redacted] gap and nominal flow
- 1thruC_11.5MW_36SSlowF - constant 11.5 MW (115%) power with [redacted] gap and low (85%) flow
- 1thruC_11.5MW_64SSlowF - constant 11.5 MW (115%) power with [redacted] gap and low (85%) flow

5a, b, f

The RELAP5 runs for the LOCA and LOPF use the following filenames and also include input and output files.

- 1thruC_10.0MW_36LOPFwV - loss of pump flow at 10 MW (100%) power with target DHRS valves
- 1thruC_10.0MW_36LOPFnoV - loss of pump flow at 10 MW (100%) power without target DHRS valves
- 1thruC_10.0MW_36LOCA1wV - loss of coolant out of reactor pool before wye at 10 MW (100%) power with target DHRS valves
- 1thruC_10.0MW_36LOCA1noV - loss of coolant out of reactor pool before wye at 10 MW (100%) power without target DHRS valves
- 1thruC_10.0MW_36LOCA2wV - loss of coolant out of reactor pool after flex line at 10 MW (100%) power with target DHRS valves
- 1thruC_10.0MW_36LOCA2noV - loss of coolant out of reactor pool after flex line at 10 MW (100%) power without target DHRS valves
- 1thruC_10.0MW_36LOCA3wV - loss of coolant in reactor pool at 10 MW (100%) power with target DHRS valves
- 1thruC_10.0MW_36LOCA3noV - loss of coolant in reactor pool at 10 MW (100%) power without target DHRS valves

[redacted]

7.2 FRAPCON Files

Four FRAPCON cases were run to provide input for the FRAPTRAN reactivity transients and the LOCA in the reactor pool. The following filenames were used with file extensions of <filename>.inp for input, <filename>.out for output, <filename>.plot for plotting, and <filename>.rst for restart which is used by FRAPTRAN.

- frapcon-36_10.0MWSS3C - constant 10 MW (100%) target irradiation with 36 μm gap
- frapcon-64_10.0MWSS3C - constant 10 MW (100%) target irradiation with 64 μm gap
- frapcon-36_600pcm3C - 115-100-115 % target power history with 36 μm gap
- frapcon-64_600pcm3C - 115-100-115 % target power history with 64 μm gap

7.3 FRAPTRAN Files

For each reactivity transient, the minimum and maximum gap between the pellet and cladding were run after 1.2 hours of operation and after three weeks of operation for a total of eight cases. The following filenames were used with file extensions of <filename>.inp for input, <filename>.out for output, and <filename>.plot for plotting.

- fraptran-36_600pcmC_bolC_NewR - 600 pcm reactivity transient with 36 μm gap at BOL conditions
- fraptran-36_600pcmC_eol_NewR - 600 pcm reactivity transient with 36 μm gap at EOL conditions
- fraptran-64_600pcmC_bol_NewR - 600 pcm reactivity transient with 64 μm gap at BOL conditions
- fraptran-64_600pcmC_eolC_NewR - 600 pcm reactivity transient with 64 μm gap at EOL conditions
- fraptran-36_30pcmpers_bolC_NewR - 30 pcm per sec reactivity transient with 36 μm gap at BOL conditions
- fraptran-36_30pcmpers_eolC_NewR - 30 pcm per sec reactivity transient with 36 μm gap at EOL conditions
- fraptran-64_30pcmpers_bolC_NewR - 30 pcm per sec reactivity transient with 64 μm gap at BOL conditions

- fraptran-64_30pcmpers_eolC_NewR - 30 pcm per sec reactivity transient with 64 μm gap at EOL conditions

FRAPTRAN was also used to assess cladding integrity during the LOCA in the reactor pool. The following filenames were used and also include input, output, and plotting files.

- fraptran-36_CladTemp_Rod17_bolC - LOCA in pool, rod 17 with [redacted] gap at BOL
- fraptran-36_CladTemp_Rod17_eolC - LOCA in pool, rod 17 with [redacted] gap at EOL
- fraptran-36_CladTemp_Rod22_bolC - LOCA in pool, rod 22 with [redacted] gap at BOL
- fraptran-36_CladTemp_Rod22_eolC - LOCA in pool, rod 22 with [redacted] gap at EOL
- fraptran-64_CladTemp_Rod17_bolC - LOCA in pool, rod 17 with [redacted] gap at BOL
- fraptran-64_CladTemp_Rod17_eolC - LOCA in pool, rod 17 with [redacted] gap at EOL
- fraptran-64_CladTemp_Rod22_bolC - LOCA in pool, rod 22 with [redacted] gap at BOL
- fraptran-64_CladTemp_Rod22_eolC - LOCA in pool, rod 22 with [redacted] gap at EOL

5a, b, f

7.4 EXCEL Files

EXCEL was used to do simple manipulations of data to prepare it for input to RELAP5, FRAPCON, and FRAPTRAN. Table 15 lists the EXCEL files generated and their purpose in the calculational scheme.

Table 15 Excel Files

EXCEL filename	Purpose
Power-profile.xlsx	Steady state power distribution
600pcm (Final) with Target.xlsx	Reactivity transient power

7.5 MATHCAD Files

MATHCAD was used to calculate the flow areas, equivalent hydraulic diameter and equivalent heated diameter for the minimum, nominal, and maximum gaps between the pellet and cladding. The following three MATHCAD files were generated:

- Areas D6_100 RevB.xmcd - minimum gap hydraulic calculations

- Areas D6_379.xmcd - nominal gap hydraulic calculations
- Areas D6_421.xmcd - maximum gap hydraulic calculations

MATHCAD was also used to calculate the minimum critical heat flux ratio using results from the LOCA and LOPF RELAP5 cases. The following two MATHCAD files were used:

- 1thruC_10.0MW_36LOCA1noV.xmcd - loss of coolant out of reactor pool before wye at 10 MW (100%) power with target DHRS valves
- 1thruC_10.0MW_36LOCA2noV.xmcd - loss of coolant out of reactor pool after flex line at 10 MW (100%) power without target DHRS valves
- 1thruC_10.0MW_36LOCA3noV.xmcd - loss of coolant in reactor pool at 10 MW (100%) power without target DHRS valves
- 1thruC_10.0MW_36LOPFnoV.xmcd - loss of pump flow at 10 MW (100%) power without target DHRS valves

Text files containing the RELAP5 data for select time points are as follows:

- 1thruC_10.0MW_36LOCA1noV_022.txt - at time 0.22 sec
- 1thruC_10.0MW_36LOCA1noV_030.txt - at time 0.30 sec
- 1thruC_10.0MW_36LOCA1noV_038.txt - at time 0.38 sec
- 1thruC_10.0MW_36LOCA2noV_022.txt - at time 0.22 sec
- 1thruC_10.0MW_36LOCA2noV_030.txt - at time 0.30 sec
- 1thruC_10.0MW_36LOCA2noV_038.txt - at time 0.38 sec
- 1thruC_10.0MW_36LOCA3noV_022.txt - at time 0.22 sec
- 1thruC_10.0MW_36LOCA3noV_030.txt - at time 0.30 sec
- 1thruC_10.0MW_36LOCA3noV_038.txt - at time 0.38 sec
- 1thruC_10.0MW_36LOCA3noV_040.txt - at time 0.40 sec
- 1thruC_10.0MW_36LOCA3noV_050.txt - at time 0.50 sec

- 1thruC_10.0MW_36LOCA3noV_060.txt - at time 0.60 sec
- 1thruC_10.0MW_36LOCA3noV_070.txt - at time 0.70 sec
- 1thruC_10.0MW_36LOCA3noV_080.txt - at time 0.80 sec
- 1thruC_10.0MW_36LOCA3noV_090.txt - at time 0.90 sec
- 1thruC_10.0MW_36LOCA3noV_100.txt - at time 1.00 sec
- 1thruC_10.0MW_36LOPFnoV_000.txt - at time 0.00 sec
- 1thruC_10.0MW_36LOPFnoV_030.txt - at time 0.30 sec

8 REFERENCES

1 Missouri University Research Reactor (MURR) Safety Analysis Report, Vols. 1 and 2, August 18, 2006.

2 "Written communication as specified by 10 CFR 50.4(b)(1) regarding responses to the "University of Missouri at Columbia – Clarifications Need to Nuclear Regulatory Commission Staff Request for Additional Information Regarding the Renewal of Facility Operating License No. R-103 for the University of Missouri at Columbia Research Reactor (TAC No. ME1580)," dated December 17, 2015," letter from John L. Fruits to U.S. Nuclear Regulatory Commission, February 8, 2016.

3 RELAP5/MOD3.3 Code Manual (NUREG/CR-5535/Rev P3-Vol I - VIII), March 2006.

4 Geelhood, K. J., et al., "FRAPCON-4-0: A Computer Code for the Calculation of Steady-State, Thermal-Mechanical Behavior of Oxide Fuel Rods for High Burnup," PNNL-19418, Vol. 1, Rev. 2, September 2015.

5 Geelhood, K. J., et al., "FRAPTRAN-2.0: A Computer Code for the Transient Analysis of Oxide Fuel Rods," (PNNL-19400, Vol.1 Rev.2), May 2016.

Attachment 7

GENERAL ATOMICS
P.O. BOX 85608 SAN DIEGO, CA 92186-5608 (858) 455-3000